ENVIRONMENTAL RESEARCH CORPORATION

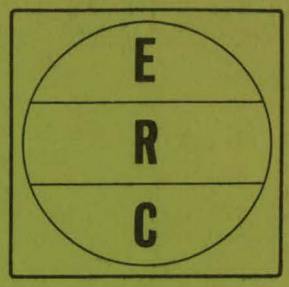

ALEXANDRIA • VIRGINIA

DISCLAIMER

NVO-1163-157

IDENTIFICATION OF ELASTIC WAVE TYPES ON SEISMOGRAMS FROM UNDERGROUND NUCLEAR EXPLOSIONS

by

W.W. Hays

October 15, 1968

Environmental Research Corporation
813 N. Royal Street
P.O. Box 1061
Alexandria, Virginia

Prepared under
Contract AT(29-2)-1163
for the
Nevada Operations Office
U.S. Atomic Energy Commission

TABLE OF CONTENTS

LIST OF ILLUSTRATIONS

ABSTRACT

The seismogram from an underground nuclear explosion represents the end result of a system composed of complex physical processes. The characteristics of the ground motion recorded on the seismogram are directly related to the characteristics of the elastic waves which propagate from the source of the explosion through the earth's crust to the seismograph.

Travel time information, particle motion diagrams (hodographs) and the radial-vertical component product waveform obtained from an analog computer operation all provide useful information which can be used to identify elastic wave types on a seismogram. Travel time data provide information on the prppagation velocity of the direct and refracted P waves, the parameters of the sequence of layers comprising the earth's crust, and an estimate of the first order on the expected arrival time of S waves having corresponding travel paths. Particle motion diagrams provide a graphic illustration of the actual particle motion recorded and permit a comparison with the particle motion expected for a specific elastic wave type. The radial-vertical component

product waveform provides a quick and practical means for identifying P, SV, and Rayleigh waves on most seismograms. In all cases, the certainty of the identification is improved through use of the product waveform, for it is based on the most diagnostic characteristic of an elastic wave, its particle motion.

Examples of typical seismograms recorded from the Boxcar and Faultless events illustrate the complex signature which the heterogeneous nature of the earth's crust imposes on the seismic waveform. The radial-vertical component product waveform deviates substantially in most cases from the ideal waveform expected from theory. Also, the frequency content shifts noticeably from higher to lower frequencies with increase in time on the seismogram.

Several studies related to the identification of elastic waves on seismograms of underground nuclear explosions are planned for the future. The objective of these studies is to develop the capability to predict the characteristics of the ground motion expected at a station in terms of specific elastic wave types.

CHAPTER 1

INTRODUCTION

The ground motion measured at a seismograph station is the result of a number of complex physical processes. These processes begin at the source of an earthquake or with the detonation of a nuclear explosive and culminate at the seismograph station with the recording of the ground motion waveform.

The objective of this report is to relate the observed ground motion on a nuclear explosive generated seismogram to specific elastic waves, i.e., body (P and S), and surface (Rayleigh and Love) waves. In a finer sense, the objective is to correlate the characteristics of observed ground motion with a body wave having a specific travel path within the earth's crust; as for example, a direct wave path, a reflected wave path, and a critically refracted wave path.

Attainment of these objectives is dependent upon the ability to identify specific elastic waves and to correlate this information with available geological and geophysical information about the crust of the earth. Fortunately, the seismogram itself contains information which is useful both in the identification process and in the definition of the

parameters of the earth's crust. Part of this information can be deduced from the first arrival times. The first arrival times from any one event recorded by a group of seismograph stations distributed over an adequate distance range can be interpreted to provide the following information:

1. The nature of the first arrival; i.e., whether it is a direct P wave or a P wave critically refracted from the Mohorovicic (M) discontinuity.

2. The propagation velocity of the P waves.

3. The thickness of the crustal layers.

4. The critical distance; i.e., the distance from the shot where the critically refracted and the direct P waves arrive simultaneously and then change their order of arrival.

5. An estimate of the first order on the expected arrival times of the S waves.

Identification of specific elastic waves is facilitated by combined use of travel time data and particle motion diagrams. An analog computer technique which exploits the

component particle motion characteristics, known to exist in theory and in practice, for the various wave types is useful for increasing the rapidity and objectivity of the identification process.

The following chapters describe various topics related to the problem of identification of elastic waves on seismograms from underground nuclear explosions. Chapter 2 reviews some of the important facts of theoretical, experimental, and observational studies of elastic waves. Chapter 3 describes the analog computer process which was used to facilitate identification as well as the use of travel time data in the identification process. Chapter 4 presents examples of elastic wave identification on seismograms of recent nuclear events. A summary of the results and future directions of study are given in Chapter 5.

CHAPTER 2

GENERAL BACKGROUND AND THEORY

2.1 THE TRANSMISSION SYSTEM OF THE EARTH

The ground motion recorded at a seismograph station from an underground nuclear explosion is the net result of a number of complex physical processes. These physical processes take place mainly in the crust and upper mantle of the earth when the source-receiver distance is small, i.e., less than 1000 km. Although difficult to generalize, these processes may be classified as occurring in three main areas: 1) the non-linear region in the immediate vicinity of the source, 2) the seismic or elastic wave transmission region, and 3) the receiver and near surface area. Physical processes which occur in these three areas are illustrated schematically in Figure 2-1 and may be described in a general way as individual parameters of a lumped parameter transmission system. The parameters may be listed as follows:

1. The source - the nuclear explosion produces a signal which is close to the ideal Dirac delta function; that is, a sharp impulsive disturbance with enormous amplitude. A delta function has a white amplitude spectrum; i.e., all frequencies are present with the same amplitude.

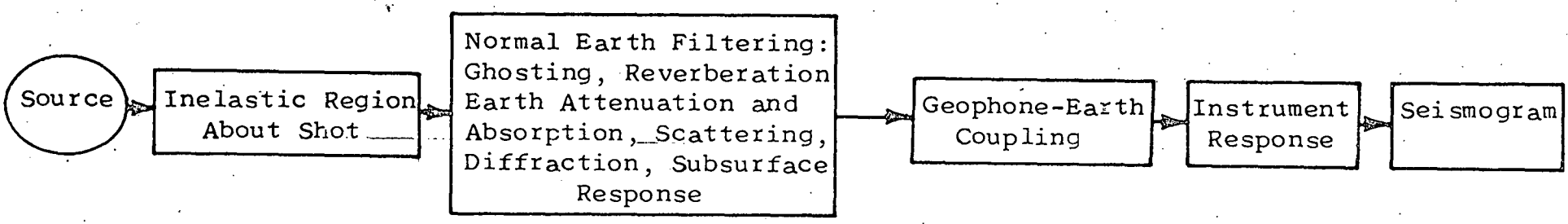

System Parameter	Individual Parameter Frequency Response	Cumulative Effect on Pulse
Explosion (Pressure)	A, F	TIME
Region Near Shot	Non-Linear	
Normal Earth Filtering	A, F	
Geophone-Earth Coupling	A, F	
Instrument Response	A, F	

Figure 2-1. Schematic Diagram of Parameters of the Transmission Model of the Earth and the Effect of Each parameter on a propagating pulse.

Environmental Research Corporation
Alexandria, Virginia

2. The inelastic region about the source - Immediately surrounding the explosion and extending radially outward for a distance, the rock behavior is extremely non-linear and complex. Approximately 50% of the available energy immediately feeds a shock wave which propagates radially outward from the wall of the shot cavity. The detailed characteristics of the intense shock wave are a function of the explosive yield as well as the cavity geometry and the properties of the rock medium in which wave propagation takes place. These characteristics are complex and are the subject of continuing research by many scientists such as Bishop (1963), Holzer (1965), Cassity (1966), Cherry (1966), and Reily (1967). As the shock wave propagates to sufficiently great radial distances, the dissipative characteristics of the rock reduce the loading intensity to the point where the elastic properties of the medium begin to play a significant role.

3. Normal earth filtering - As the wave propagates into the seismic or elastic region, less than 5% of the original energy is generally available to propagate as elastic waves. As the signal propagates over a distance of a few km, the basic seismic pulse changes shape; i.e., it

broadens in time, and decays in amplitude as a consequence of the earth's transmission characteristics. Although the explosion generates a very wide band of frequencies, differential frequency attenuation and absorption by the earth reduces the transmitted disturbance to a rather limited frequency band. As a result, the signal is transformed into a dispersed, oscillating wavelet. As the disturbance propagates through the earth, it encounters many major and minor geological boundaries. At each boundary with an acoustic impedance contrast, the energy is in part reflected and in part refracted; hence, a great variety of different transmission paths are generated. Other physical phenomena such as wave mode conversion, ghosting, (ghost energy travels upward from the source and then is reflected from the surface), reverberation within and between layers, scattering, and diffraction may occur along each transmission path and compound the complexity of the total process. Processes such as ghosting and reverberation introduce a high degree of complexity in the amplitude spectrum. Scattering causes attenuation which increases rapidly with decrease in wave length of the pulse. This action along with frequency dependent absorption causes the earth to act as a low-pass filter to seismic signals.

4. Geophone-earth coupling - The coupling between the geophone and the ground is a resonant system. The effect of the resonant system is the same as a filter; each recorded component of motion is distorted and time shifted as a direct function of the degree of coupling achieved in the emplacement of the seismograph. Usually this effect is negligible if the seismograph is carefully emplaced on a concrete pad.

5. Instrument response - The movement of the free surface of the earth is measured with a seismograph having a restricted bandwidth. This means that the output of a seismometer is a distorted version of the actual movement of the free surface. Noise on the seismogram which is unrelated to the nuclear source and the earth's subsurface response also tends to complicate the instrument response. Noise consists of disturbances which are random in both amplitude and phase as well as disturbances having identifiable coherent properties. The random noise is made up of wind noise and noise related to cultural activities. Coherent noise is introduced by the recording and data processing systems.

6. The seismogram - The signal received at a seismometer is not a single wavelet, such as would be produced

if there were only one travel path, but it represents the superposition of wavelets from all the different transmission paths possible within the crust of the earth. In addition, noise related to wave groups arriving from random directions, such as near-surface waves impinging upon randomly-located near-surface inhomogeneities, is present. The seismogram therefore, may be thought of as representing the totality of response to impulses, each impulse being associated with a disturbance that has traveled a certain path in the crust and upper mantle by reflections and refractions. That is, the impulse produced by the nuclear explosion gives rise to a traveling wavelet for each transmission path, where the shape of the wavelet is determined by the nature of the absorption spectrum of the earth for the particular path. The recorded seismogram represents the superposition of all these wavelets.

2.2 WAVES IN HOMOGENEOUS, ISOTROPIC, AND ELASTIC MEDIA

It is well known from elastic wave theory that many complicated physical processes take place between the time the propagating energy from an underground nuclear explosion first enters the elastic (seismic) region and the time it is recorded at the seismograph station. Investigators

such as Ewing, Jardetsky, and Press (1957), Bullen (1959), Grant and West (1965), and many others have reported theoretical, experimental, and observational findings which provide insight into the physical processes taking place. Some of the basic background established by these scientists necessary for understanding of elastic waves will be reviewed below.

Three basic assumptions about the earth are made in classical elastic wave theory. These assumptions are that the earth material is isotropic, homogeneous, and perfectly elastic. The assumption of isotropy considers each element of volume of the earth to have the same elastic constants and properties in all directions throughout the volume. Homogeneity implies that each element of volume is exactly like every other element of volume. An elastic solid is one in which the components of strain are homoegeneous linear functions of the stress components; i.e., the strain at any point is determined by the stress at that point.

2.2.1 Body Waves

If the medium is infinite, homogeneous, isotropic, and perfectly elastic, the equation of motion may be written

(Grant and West, 1965, p. 29) in vector form for a rectangular coordinate system as

$$\rho\ddot{\vec{u}} = (\lambda + 2\mu)\,\vec{\nabla}\theta + \mu\nabla^2\,\vec{u} \qquad (1)$$

where θ is the cubic dilatation (change in volume per unit volume), $\vec{u}$ is the displacement of a point $P(x,y,z)$, ρ is the density of the element of volume, $\ddot{\vec{u}}$ is the acceleration of a point $P(x,y,z)$ at any instant of time, λ and μ are Lame's constants (elastic moduli), $\vec{\nabla}$ is the vector differential operator

$$\left(\frac{\partial}{\partial x}\,\vec{i} + \frac{\partial}{\partial y}\,\vec{j} + \frac{\partial}{\partial z}\,\vec{k}\right)$$

and ∇^2 is the Laplacian operator

$$\left(\frac{\partial^2}{\partial x^2} + \frac{\partial^2}{\partial y^2} + \frac{\partial^2}{\partial z^2}\right)$$

If we take the divergence of both sides of equation (1) and rearrange the orders of differentiation, we obtain

$$\rho\,\frac{\partial^2\theta}{\partial t^2} = (\lambda + 2\mu)\nabla^2\theta \qquad (2)$$

Equation (2) is the standard wave equation for the propagation of cubic dilatation with a velocity,

$$\propto = \sqrt{\frac{\lambda + 2\mu}{\rho}} \qquad (3)$$

The solution demonstrates that compressional (P) waves can be propagated through any homogeneous, isotropic, and elastic solid.

If we take the curl of both sides of equation (1), we obtain

$$\rho \frac{\partial^2}{\partial t^2} (\vec{\nabla} \times \vec{u}) = \mu \nabla^2 (\vec{\nabla} \times \vec{u}) \qquad (4)$$

which once again is the standard wave equation, this time for the propagation of a pure rotational disturbance with velocity given by

$$\beta = \sqrt{\frac{\mu}{\rho}} \qquad (5)$$

This result constitutes proof of the possibility of propagating transverse or rotational (S) waves through a homogeneous, isotropic, and elastic solid.

These two types of body waves are usually referred to as P and S waves respectively. A large body of observational evidence on both wave types has been gathered by many seismologists. Some of the important characteristics of the waves are as follows:

1. P Waves - These waves have particle motion which is towards and away from the direction of propagation

(compressional). They travel with a propagation velocity which depends upon the nature of the transmission medium. A typical range of P wave velocities is 2.0 km/sec to 7.0 km/sec (Dobrin, 1960), for most materials in the crust of the earth.

2. S Waves - These waves can become plane polarized; hence, their particle motion varies. The waves are called SV if the particle motion is perpendicular to the direction of propagation and confined to the vertical plane and SH if the particle motion is perpendicular to the direction of propagation and confined to the horizontal plane. Both types of S waves have been observed on seismograms. The S waves have a propagation velocity which tends to be approximately 0.6 that of P waves for most materials in the earth's crust, (Dobrin, 1960).

2.2.2 Surface Waves

The equation of motion is completely satisfied by the solution for the P and S waves in an infinite, homogeneous, isotropic, and elastic medium. However, it is possible to write another type of solution for the equation of motion for the case in which the homogeneous, isotropic, elastic solid is bounded by a free surface. This solution corresponds to

surface waves; i.e., waves whose displacements are largely confined to the neighborhood of the boundary of a solid. The solution was proposed first by Rayleigh in 1885 for the waves which now bear his name. His work suggested that a bounded elastic solid could propagate a wave motion which is vertically polarized along the direction of propagation and which attenuates with the depth of penetration. The propagation velocity is a function of Poisson's ratio and is approximately 0.92 the shear wave velocity of the transmitting solid (Dobrin, 1960). The velocity is non-dispersive; i.e., it does not depend upon the frequency of the disturbance. The motion of a particle at the free surface describes an elliptical path which is vertically polarized with retrograde movement (counterclockwise movement when plotted in the vertical-radial plane).

Observations have confirmed the existence of waves having the characteristics described by Rayleigh. Typical observed velocities range between 1.1-4.0 km/sec for most crustal materials (Dobrin, 1960).

Love(1911) showed that a second surface wave could exist in uniform solid surface layer over a half space. These waves are transverse horizontal (SH) waves which have

particle motion at right angles to the direction of propagation and in a horizontal plane. They are SH waveguide modes which are generated by multiple reflections of SH waves in the layer. Their propagation velocity varies, approaching the shear wave velocity of the layer for short wavelengths and the shear wave velocity of the half space for long wavelengths. The typical range of observed velocities is 1.5-4.5 km/sec (Dobrin, 1960) for most materials of the earth's crust.

Love waves are more commonly observed on records of earthquakes than on records of underground nuclear explosions. Considering only conditions of symmetry, SH waves would not be expected to be generated by a point source (an explosion) in either a homogeneous or a horizontally stratified elastic medium (Grant, 1965). However, long period SH waves (Love) have been observed from some nuclear explosions, (for example, the Hardtack series, Oliver, 1960). The exact mechanism which sometimes generates SH waves from a nuclear explosion is not known at the present time. Postulated mechanisms include asymmetry of the source, wave mode conversion, and the formation of cracks around the explosion point.

2.3 THE EFFECT OF REAL EARTH MATERIALS ON ELASTIC WAVE TYPES

The assumptions of isotropy, homogeneity, and perfectly elastic behavior for the transmitting media do not generally exist in nature. Any or all of these assumptions may be violated when we deal with real seismic waves propagating through the rocks of the crust and upper mantle. The theoretical analysis of wave propagation becomes much more involved when the ideal assumptions are relaxed, and many aspects still remain to be solved. A summary of some of the known theoretical solutions reported by Ewing (1956), Bullen (1959), Grant (1965), and others is as follows:

1. Imperfectly elastic media - In media which exhibit internal viscosity or other loss mechanisms which depend upon the rate of deformation, elastic waves should be attenuated in their travel and also dispersive; i.e., have a velocity which is a function of frequency. Experimental and observational evidence, however, indicates that the loss mechanism may be of the solid friction type, a type which largely eliminates dispersion. Also, the attenuation and the changes in velocity appear to be unimportant at normal seismic wavelengths. Therefore, present evidence suggests that imperfect elastic behavior does not introduce any important modifications in the theory. P and S waves are separately identifiable.

2. Anisotropic media - In anisotropic media, the velocity with which plane elastic waves travel depends upon their direction of propagation in the transmitting medium. There are always three body waves, one of which is predominately compressional. In a transversely-isotropic medium; i.e., one which possesses two-dimensional symmetry in its elastic properties such as earth materials which have been formed by successive stages of compaction and consolidation, pure P and SV waves can be propagated only at normal or grazing incidence to the bedding plane. The waves have different values of velocity in these two directions. In all other directions of propagation, coupling between compressional and rotational motion exists. SH motions have an independent existence from the P-SV motions and will not necessarily travel with the same velocity as the SV type wave traveling in the same direction. In most earth materials, the anisotropy, if present, is not strongly pronounced. The P-SV coupling therefore is generally weak and the equations of motion separate effectively into recognizable but modified P and SV waves and a pure SH wave. The equation of motion for surface waves is more complex for propagation in transversely-isotropic media than in ideal media, however, the motion is generally very similar to the Rayleigh waves in an ideal medium.

3. Inhomogeneous media - Removal of the idealized assumption of homogeneity leads to the greatest mathematical difficulties, but the existence of velocity gradients in the earth is so commonplace that the theory can not be brought to a practical stage without consideration of the effects of heterogeneity on propagating seismic waves. Most occurrences of velocity gradients in otherwise uniform rock formations are related to the fact that materials tend to harden when subjected to compressive loads over long periods of time. This causes seismic wave velocities to increase with depth. Horizontal velocity gradients, except in unusual cases, are generally very much smaller. In heterogeneous elastic media, P and S wave motions are, in general, coupled. If the elastic properties change in the vertical direction only; i.e., vertically-inhomogeneous, the SH motion separates from the coupled P-SV motion. Pure P or SV waves exist in vertically-inhomogeneous media only when they are normally incident to the bedding planes. The distinction between P and SV motions becomes less obvious at oblique incidence, however, and "pseudo P" and "pseudo SV" waves exist. If the velocities do not change greatly within a seismic wavelength, the P and SV waves will be only very weakly coupled and will effectively separate from each other and will travel with

velocities which closely approximate the local values of α and β (equations 3 and 5) at each point in the wavefront. Thus, the trajectories will not differ significantly from what would be expected for pure P and SV waves. The equations of motion for the surface waves in isotropic, vertically-inhomogeneous media are very complex and difficult to solve except for a few special cases. The results of analyses for those cases in which rigorous solutions have been found indicates that waves of the Rayleigh type exist. These waves have a rocking sort of retrograde elliptical motion at the free surface and are highly dispersive; i.e., their velocity is a function of frequency.

4. Random Inhomogeneity - Another type of heterogeneity commonly found in the earth's crust is the uncorrelated or random type in which the elastic properties change continuously but unsystematically from point to point. Rock strata classified as single geological formations may be many hundreds of feet thick, yet their textures usually vary significantly in the scale of tens of feet. The analysis in this case is again very complex. The primary conclusion to date is that inhomogeneity which is of a random rather than of a gradual kind leads to scattering which is stronger at shorter wavelengths than

at the longer wavelengths. The scattering does not, in the first approximation, lead to P-S coupling. It does, however, band limit the frequencies that can be transmitted through any distance in the earth and provides an explanation of why real earth materials almost invariably act as a low-pass filter to seismic signals. If the medium also happens to be slightly dispersive, then the pulse velocity also changes progressively as the shorter wavelengths are eliminated. In most cases, the result is a gradual increase in propagation velocity as the pulse moves outward from the source area.

Despite significant advances made to date in understanding the physics of wave propagation, scientists are still far from being able to simulate mathematically the complex physical processes which take place during wave propagation in real earth materials. Even if the ability to do this were available, detailed information about the physical properties and spatial distribution of the subsurface rocks over a wide area is not available. As one example of man's effort to compete with existing limitations, consider the report "Computer Techniques for Tracing Seismic Rays in Two-Dimensional Geological Models" by Yacoub, et. al. (1968). This report has obvious merit, yet several limitations of the technique exist simply because man

has not yet been able to simulate the complete physical process. Some of the limitations are 1) perfect elasticity is assumed, 2) the rock units modeled are all assumed to strike perpendicularly to the plane of the source-receiver cross section, 3) the sensitivity of the ray tracing technique to the values inferred for the physical properties of subsurface layers, the source of greatest uncertainty, is unknown, and 4) the inability to simulate the physical effect of an infinite number of rays representing all possible ray paths is an unknown limiting factor.

CHAPTER 3

IDENTIFICATION OF ELASTIC WAVES ON SEISMOGRAMS

Two characteristics of the ground motion observed on a seismogram provide useful parameters for identifying specific elastic waves. These characteristics are the particle motion relationships which exist between the three components of recorded ground motion and the arrival time data. The sections which follow describe each of these parameters and their use.

3.1 COMPONENT PARTICLE MOTION RELATIONSHIPS

Most seismographs record three orthogonal componets of motion; two horizontal components (radial and transverse) and a vertical component. In many cases, the radial component is aligned with the source of the nuclear explosion before detonation so that it will record particle motion away from and toward the source in the horizontal plane. The transverse component is oriented so that it will record particle motion in the horizontal plane at right angles to that recorded by the radial component. The vertical component measures particle motion in the vertical plane. The importance of measuring three components of motion, as described, is that this procedure automatically separates certain types of elastic waves without additional transformation.

Consider the response of the radial (R) and vertical (Z) components of a seismograph and the radial-vertical component product to P, SV, and Rayleigh waves.

P Waves: A frequency component of the elastic wave motion transmitted through the earth as a P wave may be written as parametric equations of time (t) and circular frequency (ω) as follows:

$$\begin{aligned} R' &= R_o \cos(\omega t) \\ Z' &= Z_o \cos(\omega t) \end{aligned} \qquad (1)$$

where R_o and Z_o are amplitudes of the components of motion in the radial (R') and vertical (Z') directions. The output of the radial and vertical components of the seismograph, considered to be positive for ground motion away from the source and up respectively, can be written as

$$\begin{aligned} R &= GR_o \cos(\omega t - \phi) \\ Z &= \beta G Z_o \cos(\omega t - \phi - \epsilon) \end{aligned} \qquad (2)$$

where G and ϕ are the amplitude and phase response of the radial component and β and ϵ are the fractional gain and phase lag (if any) between the vertical and radial component seismometers. The product of the response of the radial and vertical components is

$$RZ = \beta G^2 R_o Z_o \cos(\omega t-\phi) \cos(\omega t-\phi-\epsilon) \quad (3).$$

Using the trigonometric identity

$$\cos A \cdot \cos B = \tfrac{1}{2}\left[\cos(A-B) + \cos(A+B)\right] ,$$

equation (3) can be written as

$$RZ = \frac{\beta G^2 R_o Z_o}{2}\left[\cos\epsilon + \cos(2\omega t-2\phi-\epsilon)\right] \quad (4).$$

Inspection of Equation (4) reveals the following facts about the radial-vertical component product waveform for the P wave:

1. The product waveform is an oscillation with twice the frequency of the incident wave. It has (neglecting the constants in front of the bracket) an amplitude of 1 and is offset from zero in the positive direction by a factor equal to $\cos\epsilon$, the cosine of the phase lag between the vertical and radial components.

2. The fractional gain factor affects only the amplitude of the product.

3. If no phase error exists ($\epsilon=0$), the product waveform is positive with an amplitude which varies from zero to +2.

If the phase error is $\pm 30^{o}$, definitely an upper limit in practice, the magnitude of the term in brackets varies from -0.13 to +1.87. This means that only about 6% negative overshoot would be expected at worst on the radial-vertical component product waveform.

SV Waves: A frequency component of the elastic motion transmitted through the earth as a SV wave has the following parametric equations;

$$\begin{aligned} R' &= R_o \cos(\omega t) \\ Z' &= -Z_o \cos(\omega t) \end{aligned} \qquad (5)$$

The vertical-radial component product response can be written, using the same instrument response constants defined above, as

$$RZ = \frac{\beta G^2 R_o Z_o}{2} \left[-\cos\epsilon - \cos(2\omega t - 2\phi - \epsilon) \right] \qquad (6)$$

Examination of Equation (6) yields the following conclusions about the product waveform for the SV wave:

1. The product waveform is an oscillation which has twice the frequency of the incident wave. It has an amplitude (neglecting the constants in front of the bracket)

of 1 and is offset from zero in the negative direction by a factor equal to cos ϵ.

2. If ϵ=0, the product waveform is negative. If the phase error is $\pm 30^{o}$, the amplitude of the term in brackets varies from +0.13 to -1.87, a positive overshoot of about 6%.

Thus, the P and SV waves have opposite sign on the radial-vertical component product waveform.

Rayleigh Wave: A frequency component of the elastic motion propagated through the earth as a Rayleigh wave has the parametric equations,

$$\begin{aligned} R' &= R_o \cos(\omega t) \\ Z' &= Z_o \sin(\omega t) \end{aligned} \qquad (7)$$

The instrument response becomes

$$\begin{aligned} R &= GR_o \cos(\omega t - \phi) \\ Z &= \beta G Z_o \sin(\omega t - \phi - \epsilon) \end{aligned} \qquad (8)$$

The product of the response of the radial and vertical components can be written as

$$RZ = \rho G^2 R_o Z_o \cos(\omega t - \phi) \cdot \sin(\omega t - \phi - \epsilon) \qquad (9) .$$

Equation (9) can be rewritten as

$$RZ = \frac{\beta G^2 R_o Z_o}{2} \left[-\sin\epsilon + \sin(2\omega t - 2\phi - \epsilon) \right] \qquad (10),$$

using the trigonometric identity

$$\sin A \cdot \cos B = \tfrac{1}{2}\left[\sin(A-B) + \sin(A+B) \right].$$

Inspection of equation (10) yields the following facts about the characteristics of the Rayleigh wave on the radial-vertical component product:

1. The gain ratio is a constant which affects only the amplitude of the product.

2. Considering the bracketed term only, the product waveform is a sine wave (when $\epsilon = 0$) which has twice the frequency of the impinging wave and which oscillates symmetrically about zero with a peak to trough amplitude of 2. For a phase error of $\epsilon = +30^o$, $\sin\epsilon = 0.5$ and the output varies from -1.5 to +0.5; that is, the output is 75% below the zero base line. For a relative phase error, $\epsilon = -30^o$, the output is 75% above the zero base line. The effect would be reversed for a wave with prograde elliptical particle motion. An error of only 6^o would produce about 10% asymmetry in the seismogram of a pure Rayleigh wave.

In summary, differences in instrument magnification do not affect the identification of P, SV and Rayleigh waves on the radial-vertical component product, but differences in the phase response do affect the ease of identification. The P and SV waves are distinctively positive and negative respectively on the radial-vertical component product waveform, if the phase error is zero. Fairly large phase errors ($\epsilon = 30^{o}$) introduce a relatively small negative or positive overshoot for the P and SV waves and do not seriously complicate the waveform. However, a small phase error ($\epsilon = 6^{o}$) produces a significant distortion in the form of the sine wave which results for pure Rayleigh waves, when $\epsilon = 0$, on the radial-vertical component product waveform.

Sutton and Pomeroy (1963) and Sutton, Mitronovas, and Pomeroy (1967) have demonstrated the applicability of the component product waveform technique for identifying elastic wave phases on seismograms of earthquakes and underground nuclear explosions. The best and most clearly defined results were obtained by the above authors for earthquake seismograms recorded at very large distances from the source. However, good results were also obtained from seismograms recorded at fairly short distances (263-1095 km) from the Hardhat event.

Figure 3-1 illustrates the analog computer circuit used to form the radial-vertical (RZ) component product waveform. The diagram for the radial-transverse (RT) and the transverse-vertical (TZ) component products would be analogous to Figure 3-1. Examples of seismograms from recent underground nuclear explosions processed with this analog computer technique are shown in Chapter 4.

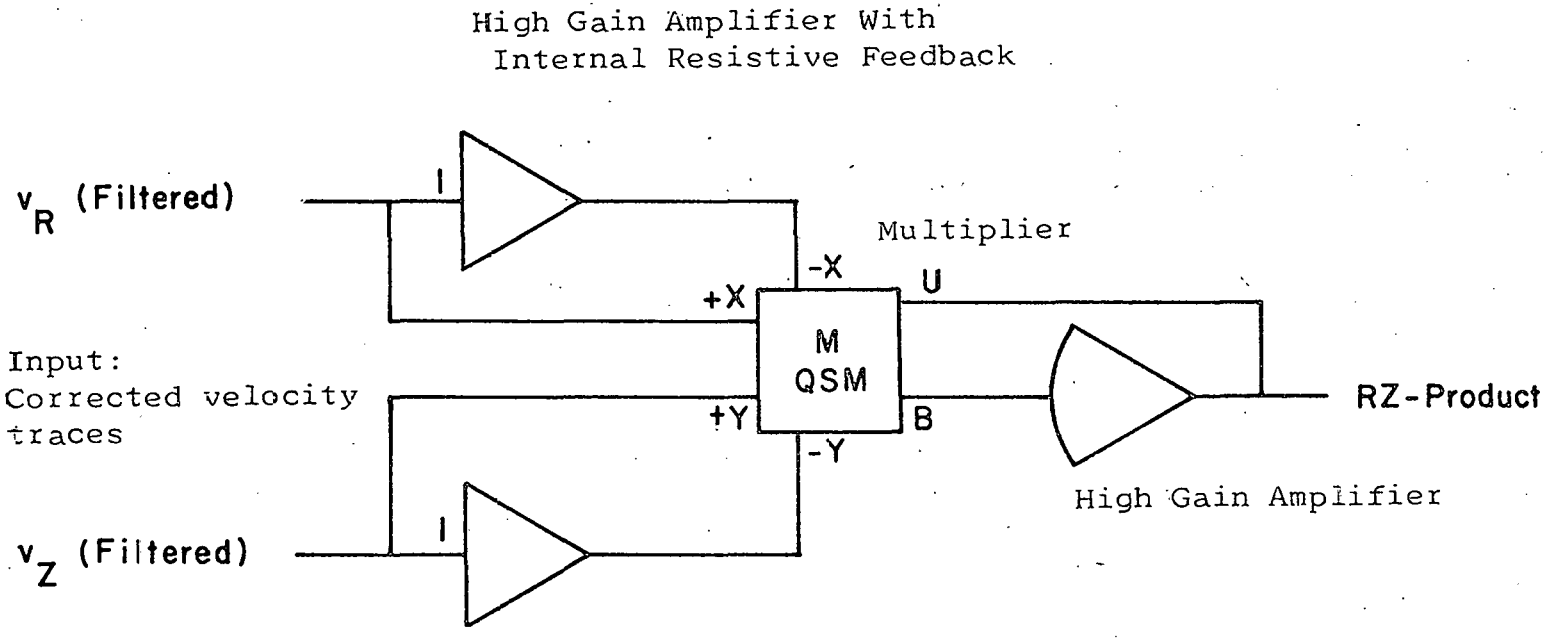

Figure 3-1. Diagram of Analog Computer Circuit Used to Form the Radial-Vertical Component Product Waveform (Lynch, 1965).

3.2 TRAVEL TIME DATA

The first-arrival time on a seismic record is the least ambiguous and the most useful travel time information on the record. The first-arrival is a P wave. The first-arrival times, when considered as a function of the distance of the recording station from the source yields information about the propagation velocity within the earth's crust and upper mantle, the depth to the crust-mantle interface (the Mohorovicic discontinuity), and specific P wave travel paths.

Figure 3-2 shows the first-arrival time as a function of station distance for the Faultless event. The travel times, despite some scatter, can be approximated closely by a two-segment, straight line, travel-time curve. The first of these segments has a best-fit equation, determined by least squares analysis, of

$$T_1(\Delta) = \left(\frac{\Delta}{5.83} + 0.39\right) \pm 0.56 \qquad (11).$$

$T_1(\Delta)$ is the travel time (sec), Δ is the station distance (km), 5.83 is the inverse slope of the line segment which corresponds to the velocity (km/sec), and 0.56(sec) is the standard error of estimate (a measure of scatter in the data). Equation (11) represents the arrival time of a P wave,

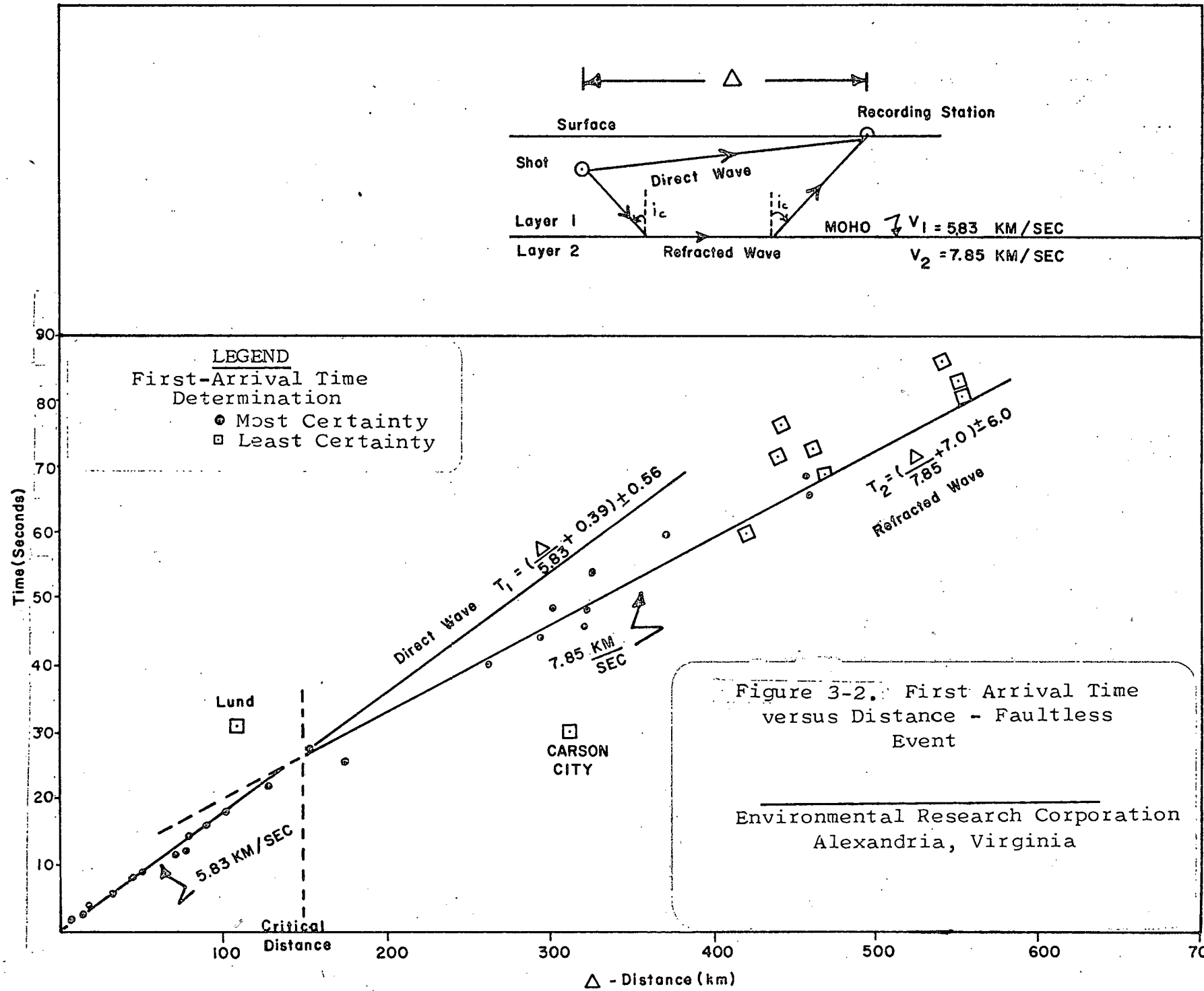

Figure 3-2. First Arrival Time versus Distance - Faultless Event

Environmental Research Corporation
Alexandria, Virginia

designated P_g in conventional earthquake terminology, which is sometimes called the "direct" wave. This wave travels exclusively in the upper layers of the crust. In reality the wave does not travel in a straight line, as shown schematically in Figure 3-2, but is refracted at a velocity interface in the upper crystalline layers of the crust. The second of the two line segments has the best-fit equation

$$T_2(\Delta) = \left(\frac{\Delta}{7.85} + 7.0\right) \pm 6.0 \qquad (12)$$

where $T_2(\Delta)$ and Δ are as defined above, 7.85 is the velocity (km/sec) and 6.0 is the standard error of estimate. Equation (12) represents the arrival time as a function of station distance for a P wave, designated P_n in conventional earthquake terminology, that has been critically refracted along the crust-mantle interface; i.e., the Mohorovicic (M) discontinuity. The refracted arrival from the M discontinuity does not exist at stations inside the distance defined by

$$\Delta_1 = \frac{V_1(2H-h)}{\sqrt{V_2^2-V_1^2}} \qquad (13)$$

where h is the depth of the shot, H is the depth to the M discontinuity, V_1 is the propagation velocity of P_g, and

V_2 is the propagation velocity of P_n. For the Faultless event, the P wave refracted from the M discontinuity arrives first at stations located more than 150 km from the source. The direct and refracted P waves arrive simultaneously at 150 km, the critical distance. The direct arrival is the first arrival at stations located less than 150 km from the source. The critical distance (Δ_c) is given for any general crust-mantle model by the formula,

$$\Delta_c = 2H\sqrt{\frac{V_2 + V_1}{V_2 - V_1}} \qquad (14)$$

where the variables are defined as above.

First-arrival times from nuclear explosions recorded over a fairly wide distance range can be used to derive a model of the earth's crust (see Dobrin, 1960, p. 69-103 for details). The basic assumptions made to generate the parameters of a crustal model are as follows:

1. The subsurface consists of a structured stack of layers having planar interfaces.
2. Each layer transmits seismic waves with a constant velocity.
3. At the interface between two layers, the seismic rays obey Snell's law.
4. Each layer has a greater velocity than the one above it.

5. The travel time is invariant to an interchange of shot point and recording station; i.e., zero dip on subsurface layer interfaces is assumed.

Figure 3-3 compares the characteristic properties of Model E derived from Faultless travel time data with four other NTS models derived by other investigators. Some of the models were derived from data obtained using detailed refraction surveys and provide more accurate information on the velocity, structural dip, and thickness of the shallow crustal layers than the models derived from travel time data exclusively from a nuclear explosion. The models all differ in 1) the number and character of shallow crustal layers, 2) the exact magnitude of the propagation velocities, and 3) the depth and structural attitude of the M discontinuity. In general, however, the parameters for all the models agree within the statistical limits of accuracy imposed by the source and the scatter in the travel time data.

The magnitude of the propagation velocity for P_g determined from Faultless travel time data is 5.83 km/sec. This value is slightly lower than the values observed by the other investigators and the value typically observed in the general area. Figure 3-4 shows the travel time data observed from 15 NTS events. The times are graded as to the certainty of the

MODEL A (NTS-Kingman, Arizona)
Diment Stewart and Roller (1961)

Thickness (km)	Compr. Vel (km/sec)	Shear Vel (km/sec)
0.67	2.30	1.30
1.60	5.20	3.00
26.60	6.15	3.50
	7.81	4.60

MODEL B (NTS-Pasadena, Calif)
Press (1960)

0.67	2.30	1.30
1.60	5.20	3.00
23.00	6.15	3.50
	7.66	4.05

MODEL C (NTS-Ordway, Colorado)
Ryall and Stuart (1963)

Thickness (km)	Compr. Vel (km/sec)
1.40	3.00
20.30	6.00
3.80	6.70
	7.90

MODEL D (NTS-Boise, Idaho)
Hill and Pakiser (1967)

1.50	2.00
20.00	6.00
10.50	6.70
	7.90

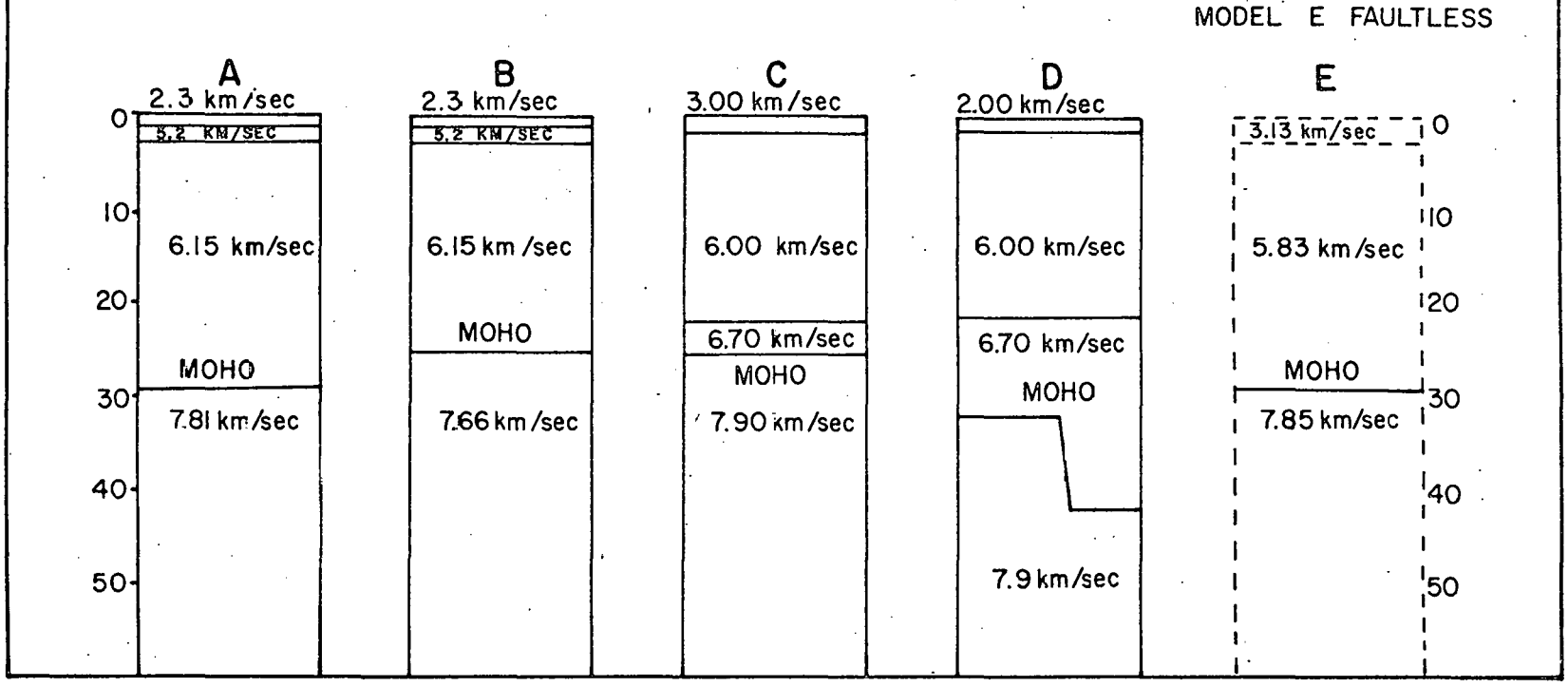

Figure 3-3. Crustal Models - NTS Area.

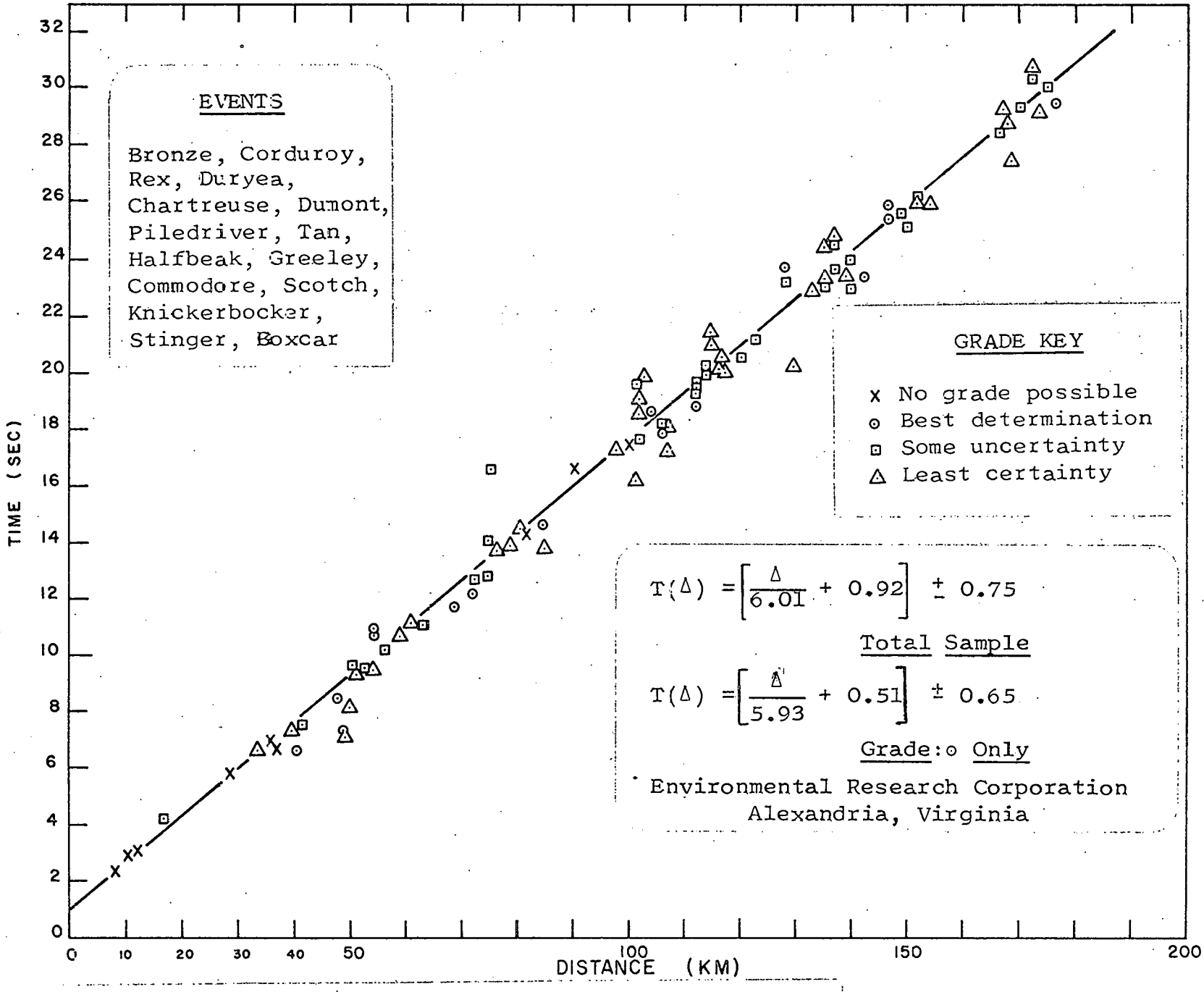

Figure 3-4. First-Arrival Times From 15 NTS Events.

determination on the record. The least squares determination of the arrival time as a function of distance for the total sample is

$$T(\Delta) = \frac{\Delta}{6.01} + 0.92 \pm 0.75 \qquad (15),$$

indicating a propagation velocity of 6.01 km/sec for P_g. If the best-determination graded samples are used, the least squares equation is

$$T(\Delta) = \frac{\Delta}{5.93} + 0.51 \pm 0.65 \qquad (16),$$

indicating a velocity of 5.93 km/sec for P_g, a difference of only 2%.

A determination of the propagation velocity of P_n is not available for most events instrumented by AEC. Faultless is the first event to be well instrumented over distances sufficiently large to allow determination of the propagation velocity of the arrival critically refracted from the M discontinuity.

Scatter is always present in the travel-time data. The scatter of the observed times about the best-fit line segments implies some uncertainty in the values of results such as propagation velocity, critical distance, and depth which are derived from the travel time data. In the analysis

of travel time data, the classical least squares model is adopted; that is, one variable is assumed to be error free. In the case of travel-time analysis, distance is assumed to be error free; that is, any error present is considered to be in the observed times.

The scatter in the observed times is physically related to four main causes: 1) occasional malfunction of the time code and high noise/signal ratio, 2) variable delay caused by surface alluvium layers, 3) departure of the earth materials along the propagation path from idealized conditions of homogeneity and isotropy, and 4) changes in the structural attitude of refraction interfaces. The magnitude of the scatter attributable to each of these causes is very difficult to ascertain accurately; therefore meaningful correction procedures are generally unavailable. An estimate of the effect of certain simple conditions can be made, however. Table 3-1 shows the calculated delaying effect which alluvium layers of different thickness have on the arrival time of a refraction from the M discontinuity recorded at different station distances. Assumed propagation velocities are 1) 2.30 km/sec - alluvium layer, 2) 5.83 km/sec - P_g, and 3) 7.85 km/sec - P_n. All layers are assumed to be horizontal. The depth of the M discontinuity is assumed to be 29.1 km.

Thickness of Alluvium Layer (km)	Arrival Time (sec) for Different Station Distances			
	Δ = 100 km	Δ = 200 km	Δ = 300 km	Δ = 400 km
0	19.26	32.00	44.74	57.48
0.5	19.38	32.12	44.86	57.60
1.0	19.51	32.25	44.99	57.73
1.5	19.63	32.37	45.11	57.85
2.0	19.76	32.50	45.24	57.98
3.0	20.00	32.74	45.48	58.42

Table 3-1

Calculated Effect of an Alluvium Layer of Different Thickness on the Arrival Time of a Refraction from the M Discontinuity

Table 3-2 shows the calculated effect of different assumed structural dips of the M discontinuity on the arrival times of the refracted wave recorded at stations located different distances in both the up and down-dip direction from the source. The propagation velocities are assumed to be 1) 5.83 km/sec - P_g and 2) 7.85 km/sec - P_n. The vertical depth to the M discontinuity is assumed to be 29.1 km beneath the shot location.

Assumed Dip of M Discontinuity (degrees)	Arrival Time (sec) for Different Station Distances		
	Δ = 100 km	Δ = 200 km	Δ = 300 km
0	19.26	32.00	44.74
1	td: 19.55	32.42	45.29
	tu: 19.14	31.62	44.08
2	td: 19.74	32.81	45.87
	tu: 18.74	31.20	43.46
3	td: 19.93	33.19	46.45
	tu: 18.73	30.78	42.83
4	td: 20.12	33.57	47.01
	td: 18.51	30.35	42.19
5	td: 20.30	33.93	47.56
	tu: 18.29	29.92	41.55

Table 3-2

Calculated Effect of Different Structural Dips of the M Discontinuity on the Arrival Time of the Refracted P Wave Recorded at Down Dip (td) and Up Dip (tu) Stations.

The crustal model, despite the simplifying assumptions made to derive it, serves a very useful purpose. It provides estimates of the first order of the important physical parameters of the complex crust of the earth, a crust which departs from the idealized assumptions in ways such as the following:

1. Deviations of layer interfaces from horizontal planes.
2. Surface irregularities and inhomogeneity.
3. Horizontal and vertical velocity gradients.
4. Velocity reversals
5. Many layers and acoustic impedance contrast interfaces.

The parameters of the derived crustal model, since they are derived from the actual data, can be used as constants to construct theoretical travel time curves as a function of station distance. These curves provide reasonable guide lines which can be used to identify, on seismograms, elastic waves having a specific travel path in the earth.

Theoretical travel time curves as a function of the station distance can be calculated for P and S waves which have traveled a direct path (P_d and S_d), a critically refracted path (P_r and S_r), and a reflected path (P_{rr} and S_{rr}). The formulae which apply for a two layer earth model are as follows:

$$T(\Delta) = \sqrt{\frac{\Delta^2 + h^2}{V_1^2}} \qquad \underline{\text{Direct Wave}} \qquad (17),$$

$$T(\Delta) = \sqrt{\frac{\Delta^2 + (2H-h)^2}{V_1^2}} \qquad \underline{\text{Reflected Wave}} \qquad (18),$$

$$T(\Delta) = \frac{\Delta}{V_2} + \frac{2H-h}{V_1}\sqrt{1 - \frac{V_1^2}{V_2^2}} \qquad \underline{\text{Refracted Wave}} \qquad (19).$$

In each formula, Δ is the surface distance (km) of the recording station from the source, H is the depth (km) to the M discontinuity, h is the depth of burial (km) of the nuclear device, V_1 is the propagation velocity (km/sec) in the crust, and V_2 is the propagation velocity (km/sec) in the mantle.

The P wave propagation velocities are determined from analysis of the first arrival times. Propagation velocities of the corresponding S waves are estimated on the basis of theoretical and observational evidence that S waves propagate with a velocity of 0.6 that of P waves for most earth materials.

Examples of elastic wave identification in terms of specific travel paths are in the Faultless report (Berry, Hays, Davis, and Lahoud, 1968). Additional examples are shown in Chapter 4.

CHAPTER 4

EXAMPLES OF ELASTIC WAVE IDENTIFICATION

4.1 RADIAL-VERTICAL COMPONENT PRODUCT WAVEFORM

Figures 4-1 through 4-16 illustrate typical particle velocity seismograms from two nuclear events, Boxcar and Faultless, recorded at distances ranging from 45.6-549.5 km. Body waves are identified on each of the seismograms in terms of a specific travel path in the earth as described in Chapter 3. In each figure, P_d and S_d correspond to the direct P and S wave respectively, P_r and S_r to the corresponding wave critically refracted along the M discontinuity, and P_{rr} and S_{rr} to the P and S wave reflected from the M discontinuity. The surface wave is identified in general terms only; although, it generally exhibits the particle motion characteristics of a Rayleigh wave, as will be discussed in section 4.2 below.

The radial-vertical component product waveform, RZ, is displayed as the bottom trace on each of the seismograms in Figures 4-1 through 4-16. As discussed in Chapter 3, RZ should display definite characteristics for elastic waves propagating in ideal media and recorded with instruments which

have little or no phase lag difference between the radial and vertical component. If the motion that is away on the radial component and the motion that is up on the vertical component are considered to represent the positive directions, RZ should display the following characteristics:

1. RZ is positive for P wave particle motion.
2. RZ is negative for SV wave particle motion.
3. RZ oscillates from positive to negative for the retrograde elliptical Rayleigh wave particle motion.

The sign convention of RZ is reversed for some of the seismograms of Figures 4-1 through 4-16. This does not affect the usefulness of the component product, however, for the P and SV waves still have opposite signs and the Rayleigh wave still is characterized as an oscillating sine wave. Records on which the polarity of RZ is reversed are labeled accordingly on each of the figures to insure proper interpretation.

Conclusions which can be drawn from Figures 4-1 through 4-16 may be summarized as follows:

1. The RZ product is useful for making quick identifications of the P, SV, and Rayleigh waves on most seismograms.

In all cases, the certainty of the identification is improved through the use of the RZ waveform, for it is based on the most diagnostic characteristic of an elastic wave, its particle motion.

2. The RZ waveform is fairly complex and deviates in most cases from the waveform expected under idealized conditions. The deviation takes the form of fairly significant positive and negative overshoots for the body waves and asymmetry of the pure sine wave expected for a Rayleigh wave. In spite of the deviation, the RZ waveform contains useful supplemental information. As described in Chapter 3, the frequency of the RZ waveform is doubled relative to that of the individual components for each wave type. Doubling the frequency tends to make the progressive frequency change, known to exist in the earth, between P, SV, and Rayleigh waves more evident to the eye on the RZ waveform. The readily apparent shift to lower frequencies with increasing time on the seismograms and the relatively narrow frequency pass band are evidence of the effect which the randomly heterogeneous crust of the earth has on a propagating wave.

3. In every case, the first motion exhibits pure P-type particle motion on the RZ waveform. The first S motion is not always clearly defined, however.

4. Surface waves having well defined, near-perfect Rayleigh wave-type motion are well displayed on many seismograms (Figures 4-1, 4-3, 4-5, 4-8, 4-12). Significant motion exists on the transverse component in every case, however, a fact that should not be true for Rayleigh waves in ideal earth media.

5. The RZ waveform is near-perfect for several stations: Tonopah Church (Figure 4-6), SE-4 (Figure 4-8), Gabbs (Figure 4-9), McGill (Figure 4-10), and Frenchman Mountain (Figure 4-12).

6. Several seismograms for stations located a fairly great distance from the source of the explosion exhibit clear separation between the various body wave arrivals on the RZ waveform. Examples are Tonopah Church (Figure 4-6), Pioche (Figure 4-12), Stateline (Figure 4-14), and Ogden (Figure 4-15). San Francisco, located the

greatest distance from the source, has a high noise background which overrides the RZ waveform and prevents clear definition.

Explanations for the general complexity of the RZ waveform is undoubtedly related to the heterogeneous nature of the earth's crust, the primary propagation medium for seismic waves recorded at distances less than 550 km. Scattering, reverberation, and lateral refraction of short period seismic energy by tectonic features of the crust are probably responsible for much of the complexity of the particle motion. Also, wave mode conversion probably is an important complicating factor. Analysis of the Faultless data (Berry et.al., 1968) suggests that converted waves exist and have fairly prominent amplitudes in many cases. Converted waves will be the subject of a future study.

Radial Component Velocity

P'_d

Transverse Component Velocity

Surface Wave

STATION: BPF 607

Δ = 45.6 Km

Faultless Event

S'_d

First Arrival Time: 8.20 sec

S'_{rr}

10 Seconds

4-6

Vertical Component Velocity

P'_{rr}

Radial-Vertical Component Product Trace

REVERSED POLARITY

Environmental Research Corporation
Alexandria, Virginia

Figure 4-1. Particle Velocity Seismogram and Radial-Vertical Component Product Waveform, Station BPF 607 - Faultless Event.

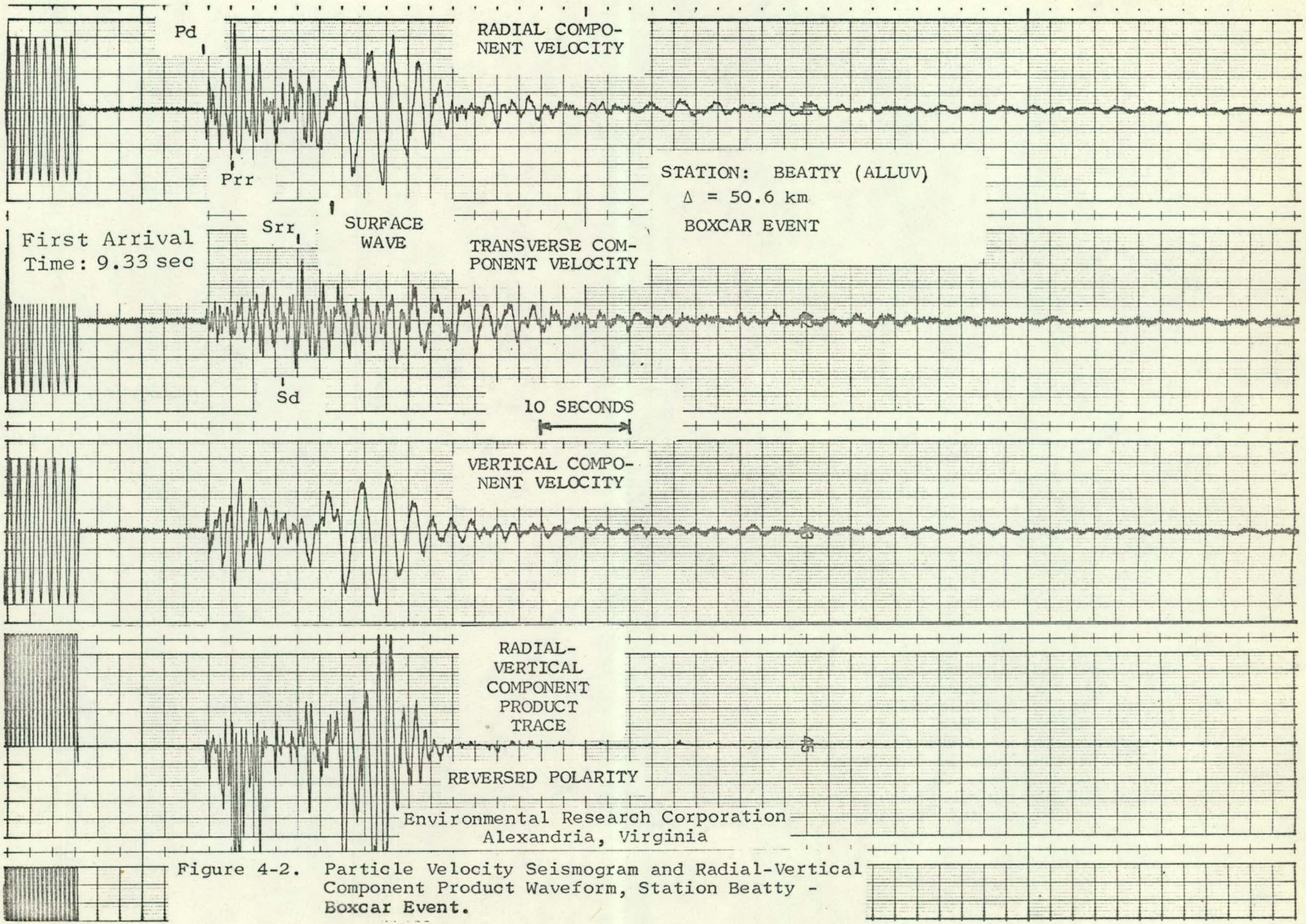

Figure 4-2. Particle Velocity Seismogram and Radial-Vertical Component Product Waveform, Station Beatty - Boxcar Event.

Radial Component Velocity

Surface Wave

P_r

P_d

P_{rr}

Station: Manhattan

Δ = 77.8 km

Faultless Event

Transverse Component Velocity

S_{rr}

First Arrival Time: 14.80 sec

S_d

S_r

4-8

Vertical Component Velocity

10 Seconds

Radial-Vertical Component Product Trace REVERSED POLARITY

Environmental Research Corporation
Alexandria, Virginia

Figure 4-3. Particle Velocity Seismogram and Radial-Vertical Component Product Waveform, Station Manhattan - Faultless Event.

SRT

STZ

Radial Component Velocity

P_r

P_d

First Arrival Time: 18.10 sec

P'_{rr}

Transverse Component Velocity

S_r

S_d

S_{rr}

Station: Eureka

Δ = 100.2 km

Faultless Event

10 Seconds

Vertical Component Velocity

Environmental Research Corporation
Alexandria, Virginia

Radial-Vertical Component Product Trace

Figure 4-4. Particle Velocity Seismogram and Radial-Vertical Component Product Waveform, Station Eureka - Faultless Event.

Figure 4-5. Particle Velocity Seismogram and Radial-Vertical Component Product Waveform, Station SE-2 - Boxcar Event.

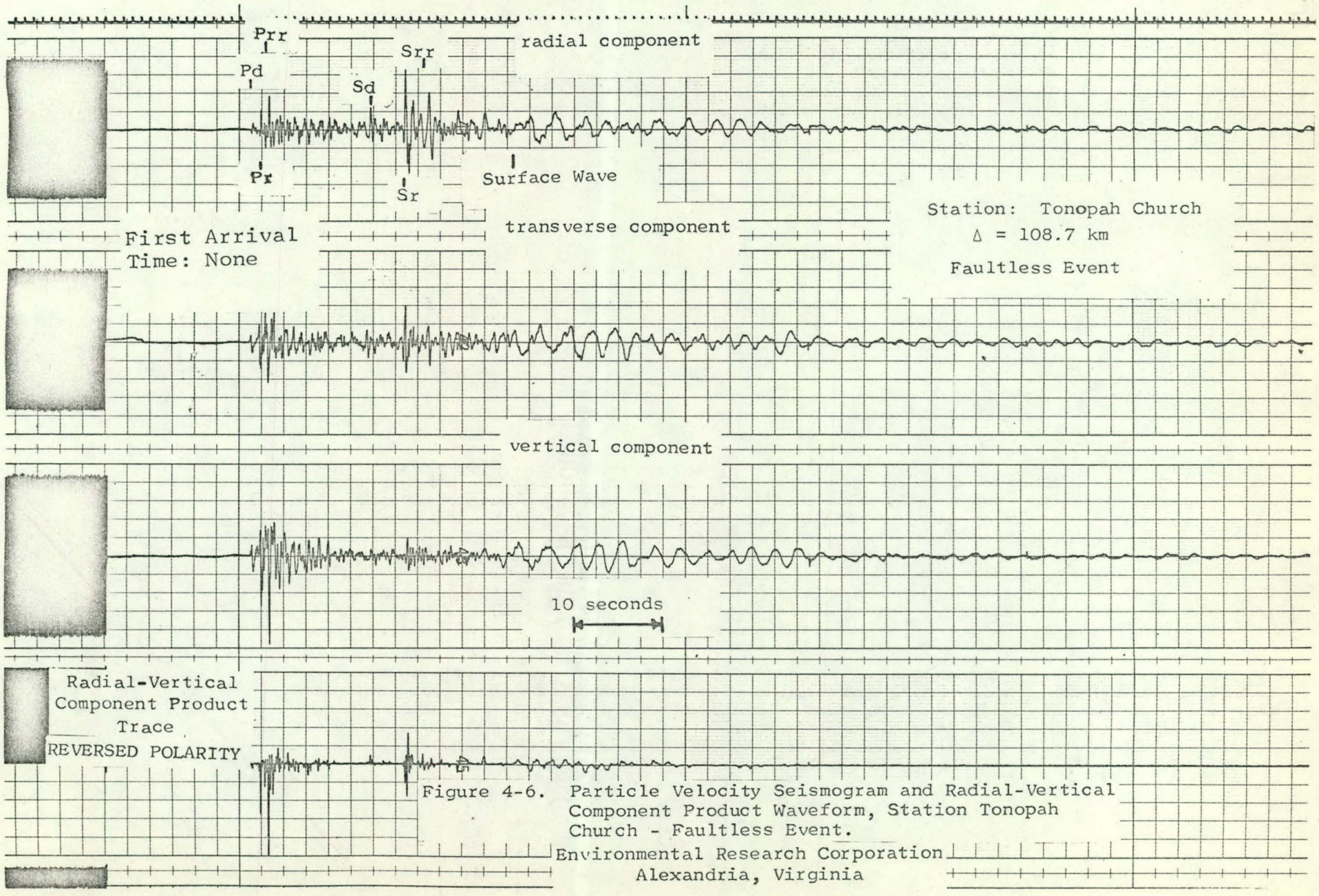

Figure 4-6. Particle Velocity Seismogram and Radial-Vertical Component Product Waveform, Station Tonopah Church - Faultless Event.

Environmental Research Corporation
Alexandria, Virginia

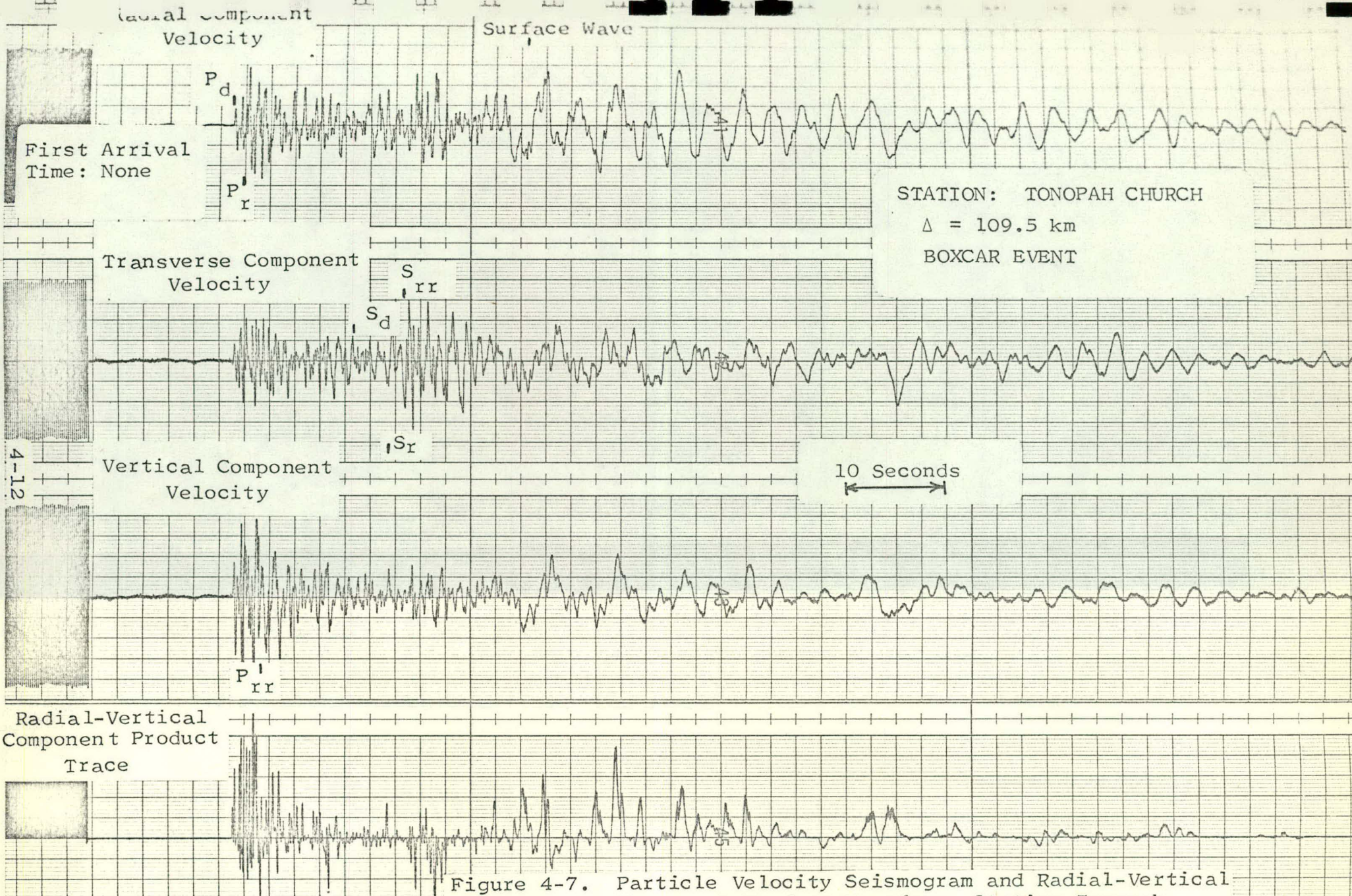

Figure 4-7. Particle Velocity Seismogram and Radial-Vertical Component Product Waveform, Station Tonopah Church - Boxcar Event.
Environmental Research Corporation
Alexandria, Virginia

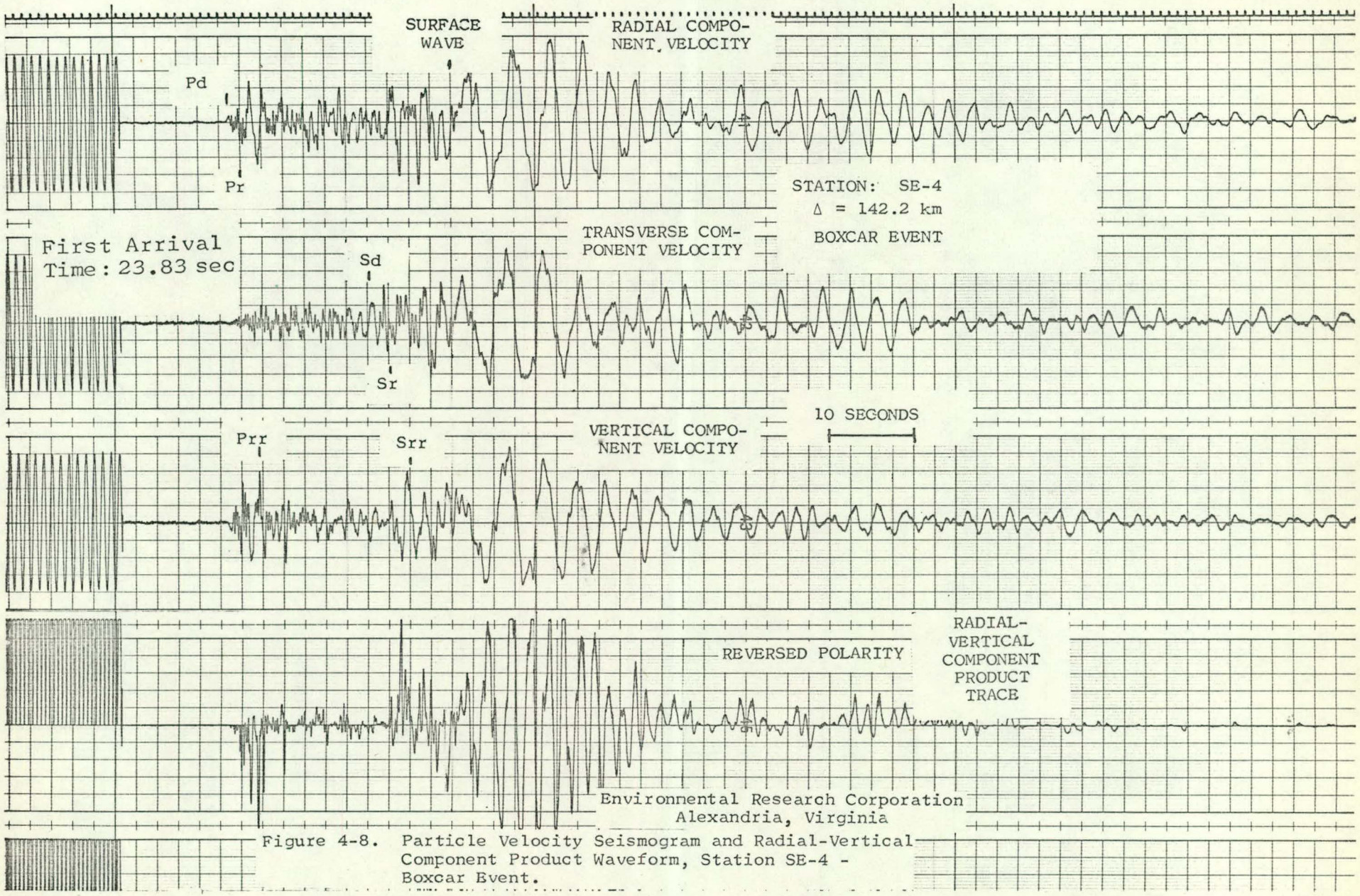

Figure 4-8. Particle Velocity Seismogram and Radial-Vertical Component Product Waveform, Station SE-4 - Boxcar Event.

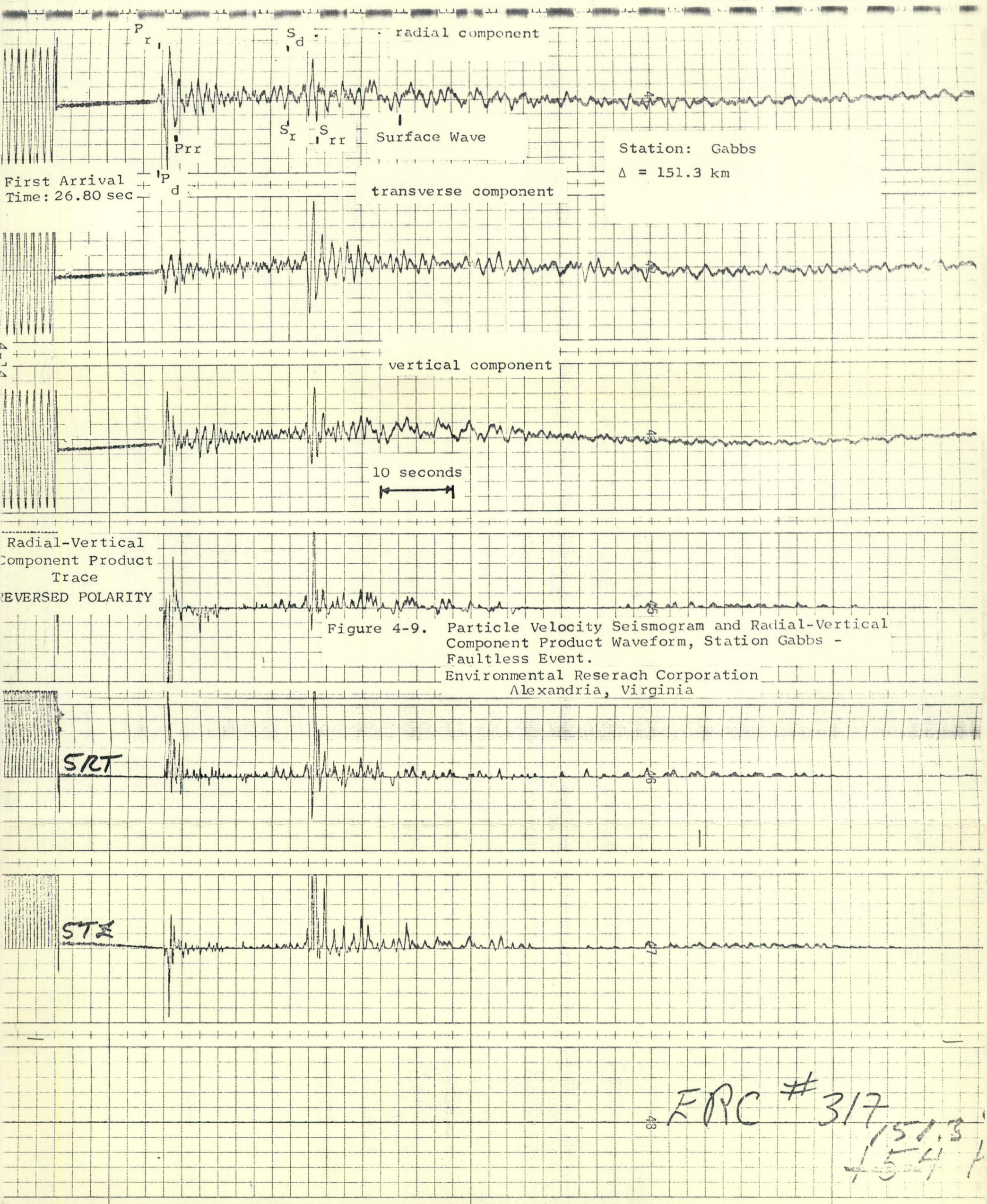

Figure 4-9. Particle Velocity Seismogram and Radial-Vertical Component Product Waveform, Station Gabbs - Faultless Event.
Environmental Reserach Corporation
Alexandria, Virginia

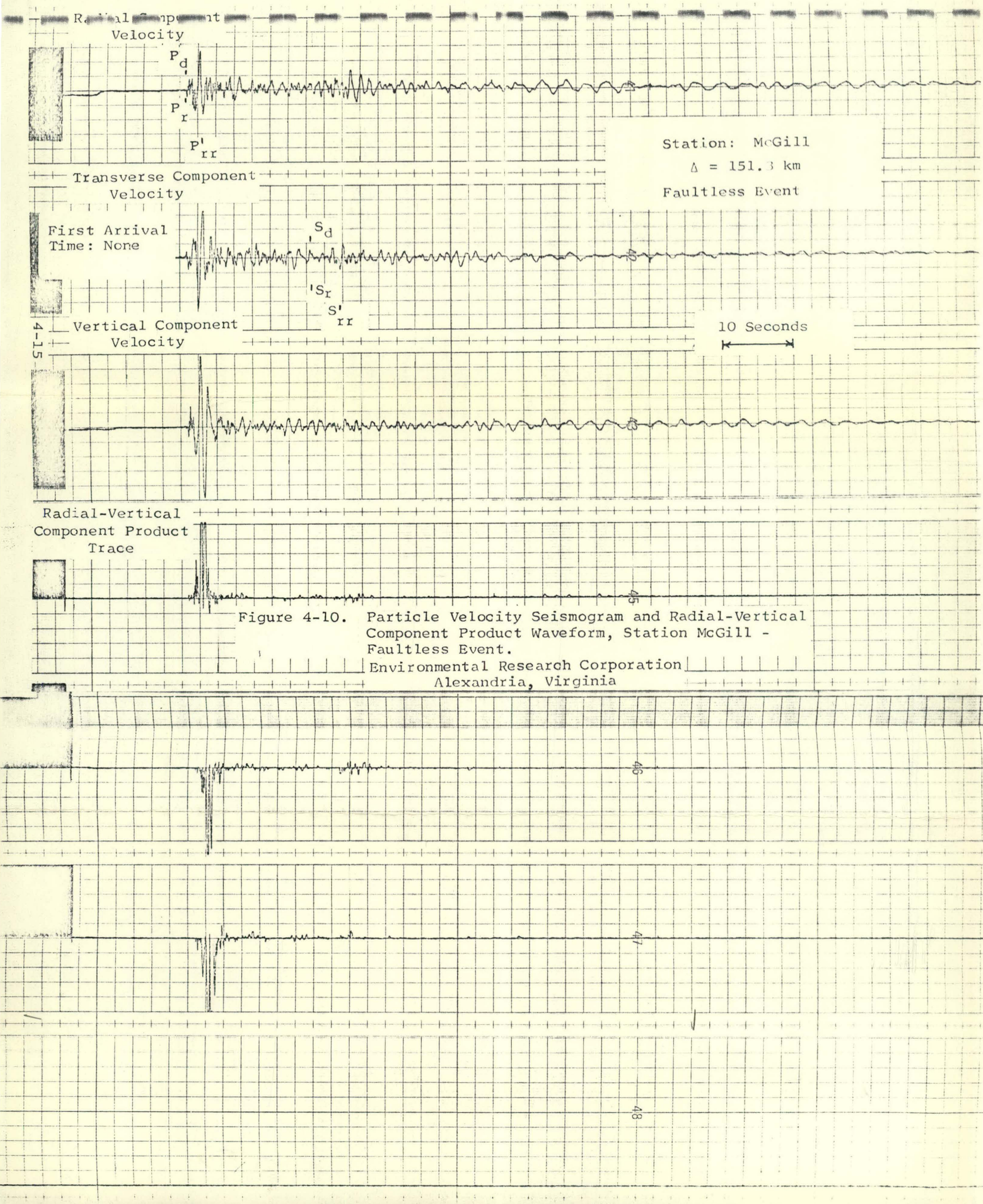

Figure 4-10. Particle Velocity Seismogram and Radial-Vertical Component Product Waveform, Station McGill - Faultless Event.

Environmental Research Corporation
Alexandria, Virginia

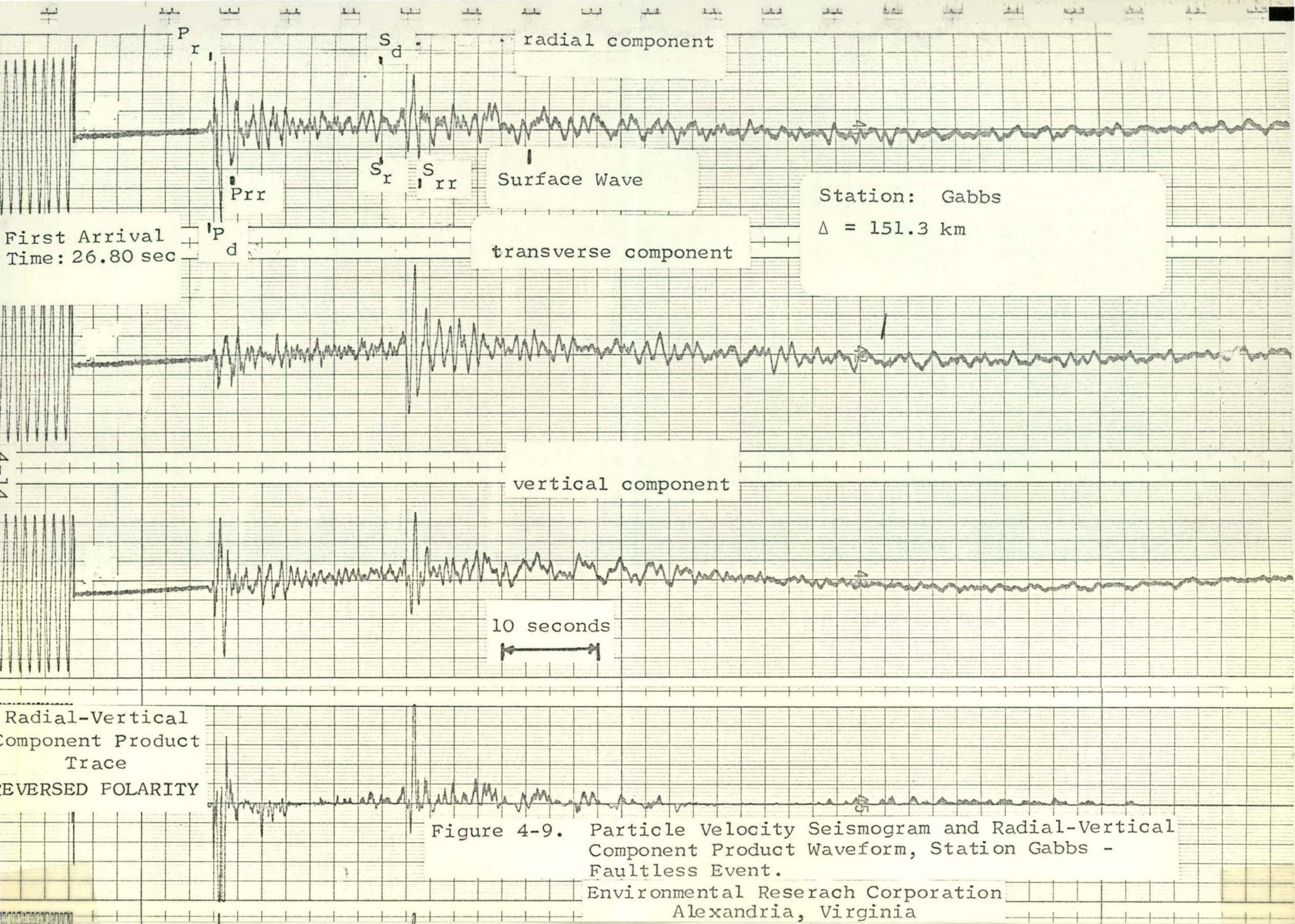

Figure 4-9. Particle Velocity Seismogram and Radial-Vertical Component Product Waveform, Station Gabbs - Faultless Event.

Environmental Reserach Corporation
Alexandria, Virginia

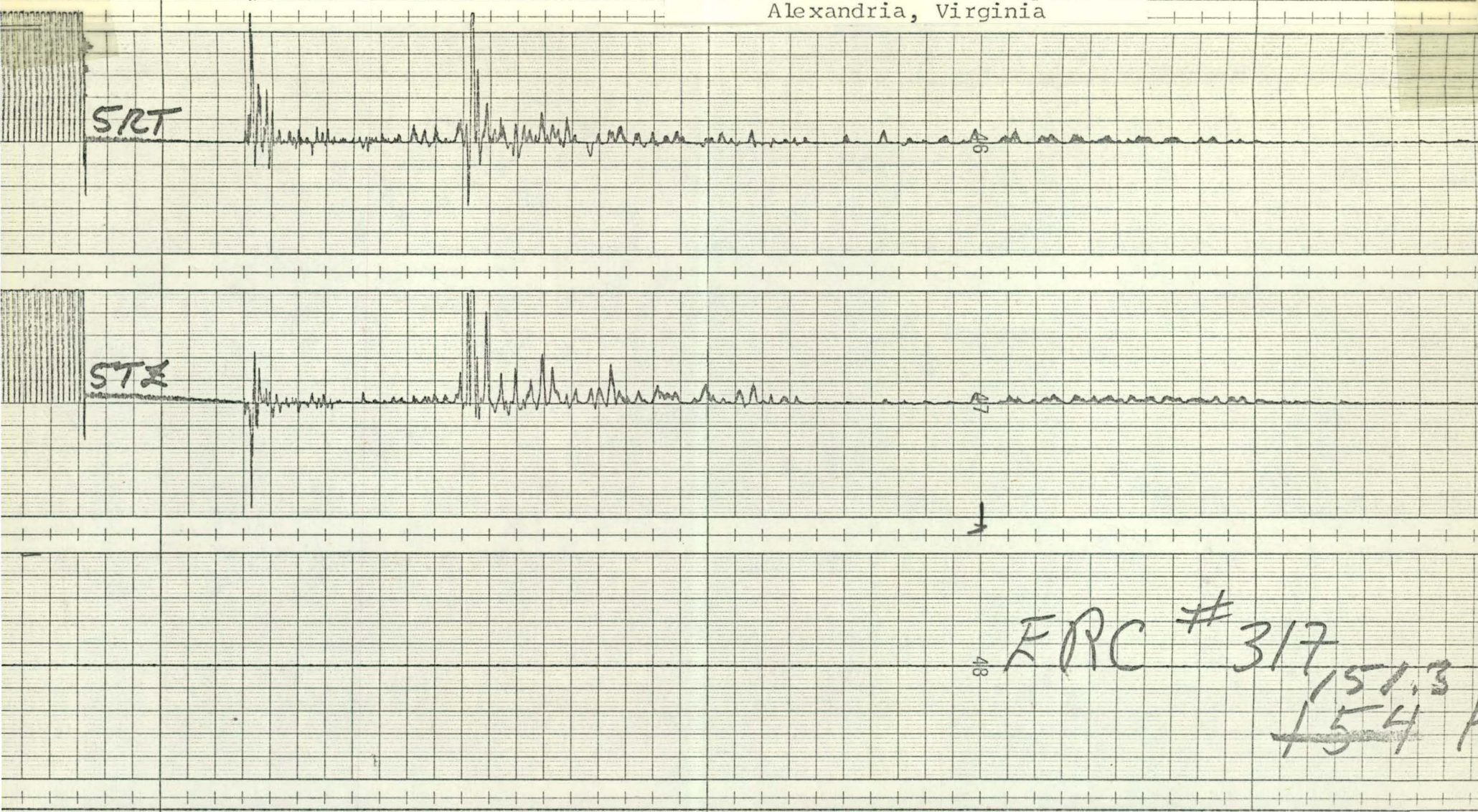

Velocity

P_d

P'_r

P'_{rr}

Station: McGill

Δ = 151.3 km

Faultless Event

Transverse Component Velocity

First Arrival Time: None

S_d

S_r

S'_{rr}

Vertical Component Velocity

10 Seconds

4-15

Radial-Vertical Component Product Trace

Figure 4-10. Particle Velocity Seismogram and Radial-Vertical Component Product Waveform, Station McGill - Faultless Event.

Environmental Research Corporation
Alexandria, Virginia

46

47

48

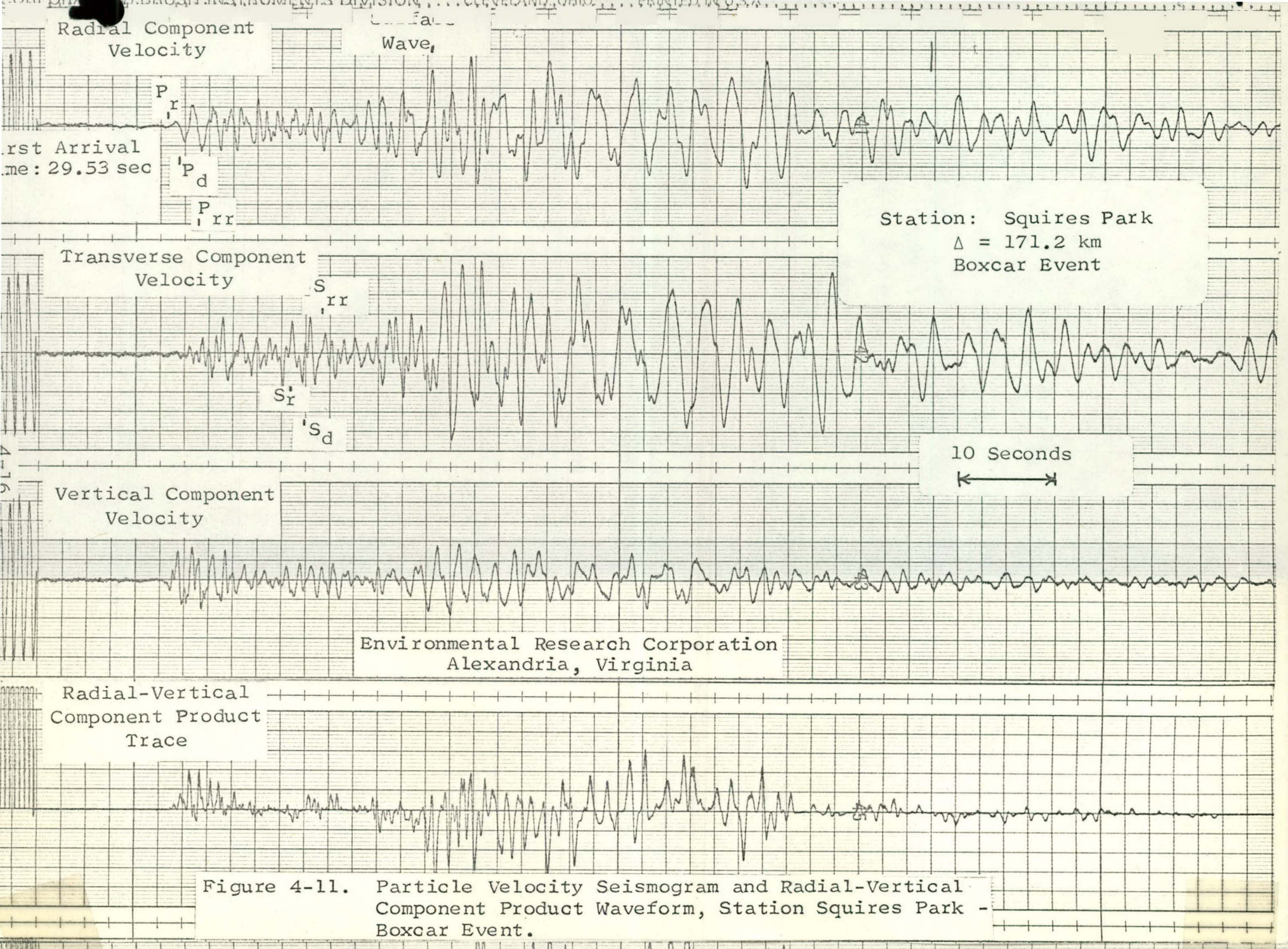

Figure 4-11. Particle Velocity Seismogram and Radial-Vertical Component Product Waveform, Station Squires Park - Boxcar Event.

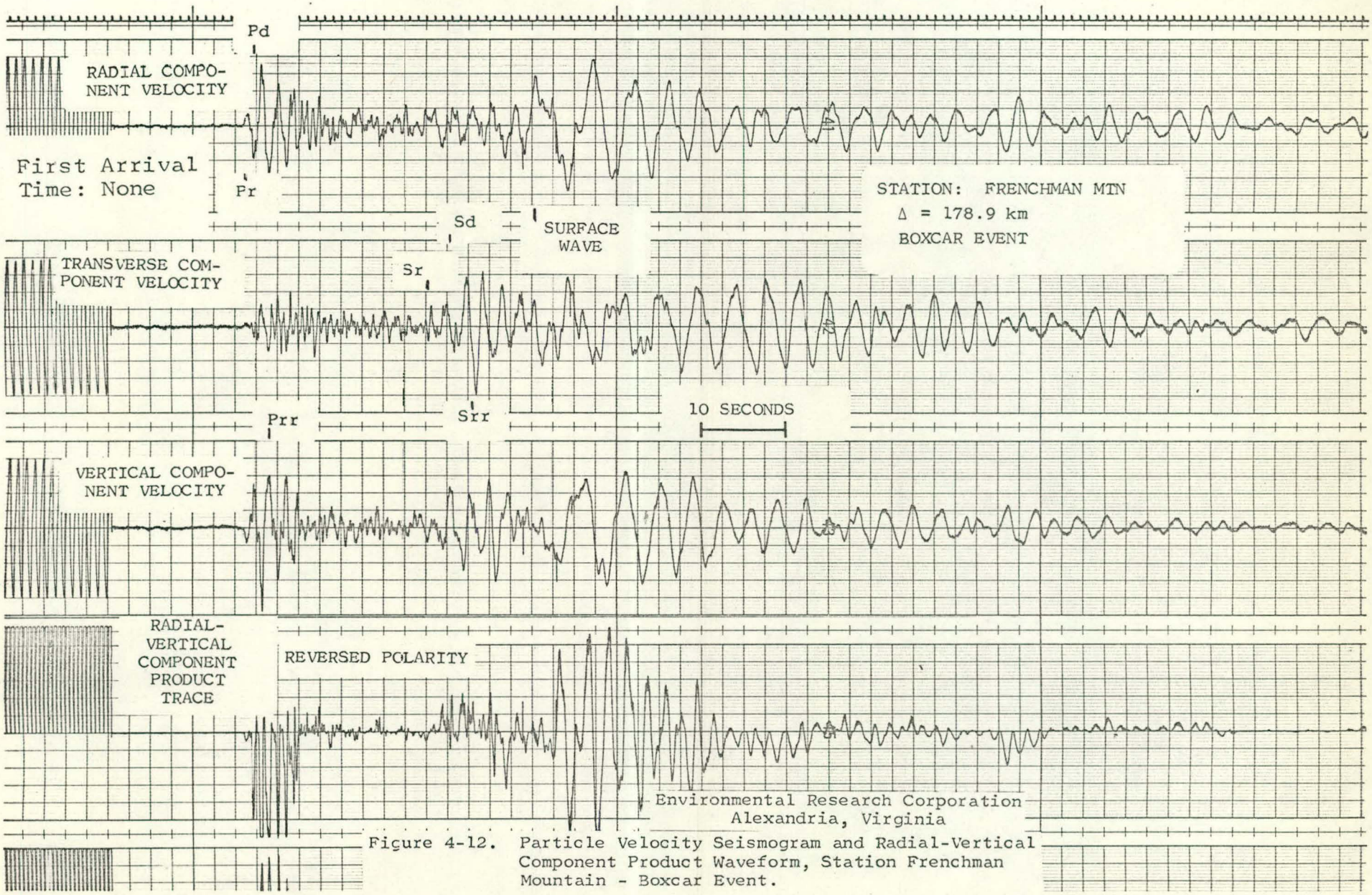

Figure 4-12. Particle Velocity Seismogram and Radial-Vertical Component Product Waveform, Station Frenchman Mountain - Boxcar Event.

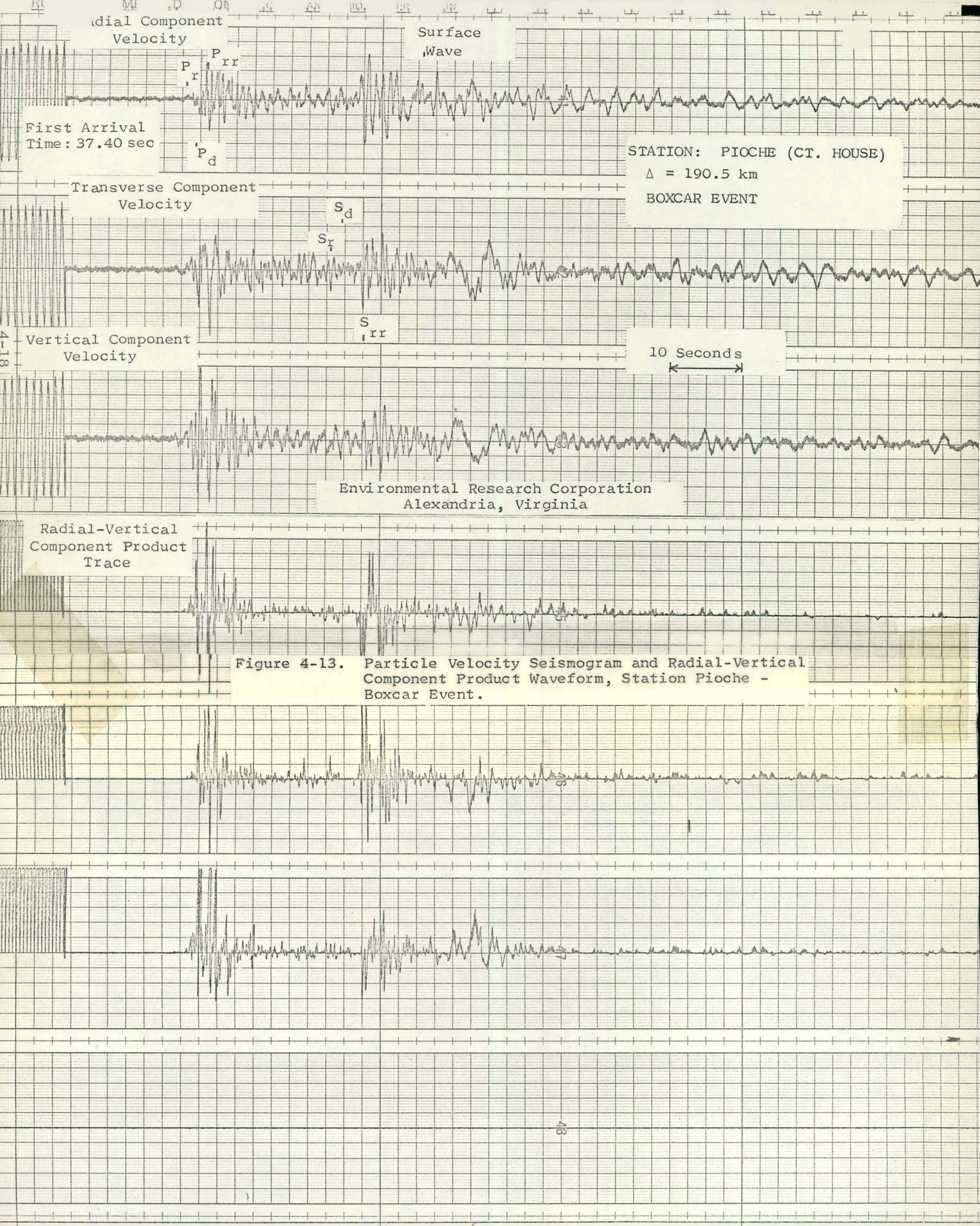

Figure 4-13. Particle Velocity Seismogram and Radial-Vertical Component Product Waveform, Station Pioche - Boxcar Event.

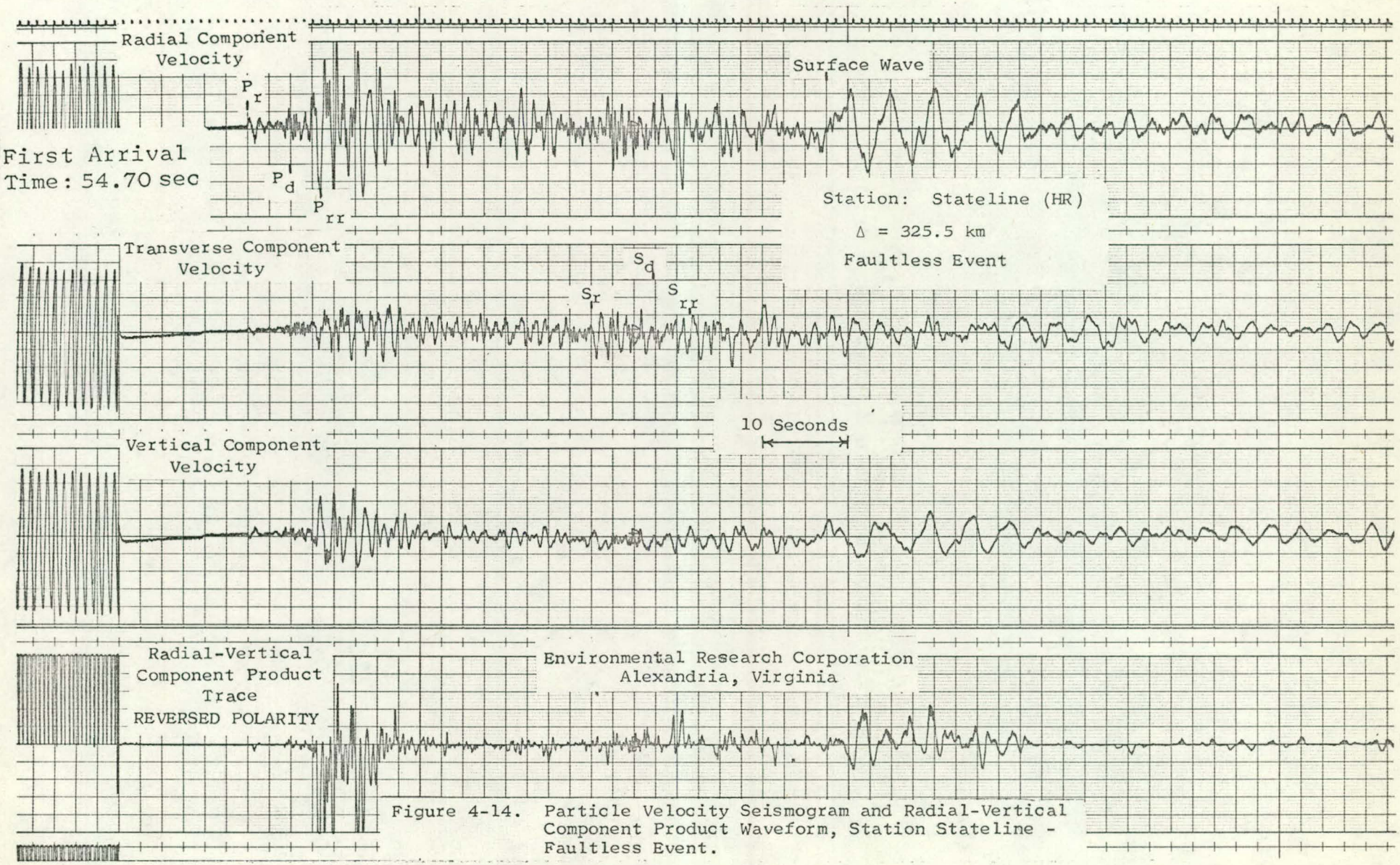

Figure 4-14. Particle Velocity Seismogram and Radial-Vertical Component Product Waveform, Station Stateline - Faultless Event.

Figure 4-15. Particle Velocity Seismogram and Radial-Vertical Component Product Waveform, Station Ogden - Faultless Event.

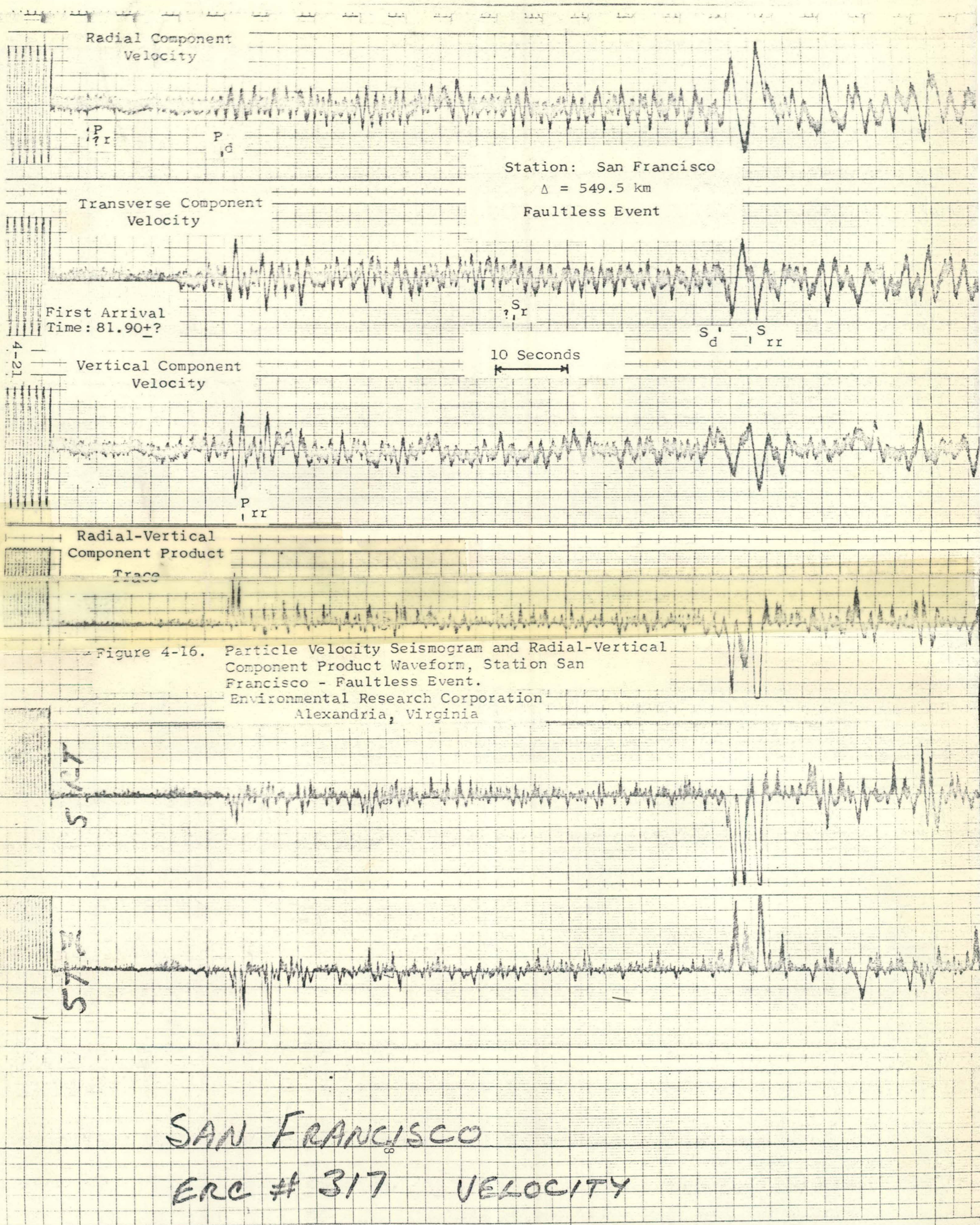

Figure 4-16. Particle Velocity Seismogram and Radial-Vertical Component Product Waveform, Station San Francisco - Faultless Event.
Environmental Research Corporation
Alexandria, Virginia

SAN FRANCISCO

ERC # 317 VELOCITY

4.2 PARTICLE MOTION DIAGRAMS

The parametric equations of the instrument response to a P wave propagating in an ideal medium are defined in Chapter 3 (equation 2). This equation may be written as

$$R = R_o \cos(\omega t) \qquad (1),$$
$$Z = Z_o \cos(\omega t)$$

where R_o and Z_o are amplitude factors and the phase lag error is assumed to be zero. Hence, a single frequency P wave has a particle motion diagram in the Z vs. R plane which traces out a straight line as a function of time. The line passes through the origin and lies in the first and third quadrants. The slope of the line varies according to the relative values of R_o and Z_o.

The parametric equation representation of the ideal SV wave, also defined in Chapter 3 (equation 5), is (for a zero phase lag between the components)

$$R = R_o \cos(\omega t) \qquad (2).$$
$$Z = -Z_o \cos(\omega t)$$

The particle motion diagram as a function of time in the Z vs. R plane for the SV wave is also a straight line passing

through the origin; however, it lies in the second and fourth quadrants.

The instrument response to an ideal Rayleigh wave has parametric equations (equation 8 in Chapter 3) which can be rewritten as follows (for zero phase lag between the components):

$$\begin{aligned} R &= R_o \cos(\omega t) \\ Z &= -Z_o \sin(\omega t) \end{aligned} \qquad (3).$$

Inspection of equation (3)reveals that the trace, as a function of time, is an ellipse with counterclockwise movement (retrograde) in the Z vs. R plane. The length of the major and minor axes of the ellipse vary in accordance with the values of R_o and Z_o. In theory, the length of the vertical axis of the particle motion ellipse for the perfect Rayleigh wave is about $1\frac{1}{2}$ times greater than the length of the radial axis.

Figures 4-17 through 4-19 illustrate particle motion diagrams (hodographs) of the displacement in the Z vs. R plane for portions of a seismogram corresponding to specific elastic waves. Figure 4-17 illustrates the particle motion of P and S waves. In general, the P wave motion is essentially

linear and largely in the first and third quadrants. The S wave motion is less linear and is primarily in the second and fourth quadrants. Deviations from these quadrants is a cause of the positive and negative overshoots observed on the RZ waveforms of Figures 4-1 through 4-16. Possible wave mode conversion is another cause. Surface wave particle motion diagrams are shown in Figures 4-18 and 4-19. The particle motion in all cases is retrograde and essentially elliptical. The orientation and eccentricity of the ellipses vary. The vertical axis is usually the major axis; although many of the axes exhibit rotation.

The combined use of particle motion diagrams, travel time data, and the RZ waveform provide a useful and practical means of identifying elastic waves on a seismogram. These techniques utilize the basic information contained on the seismogram.

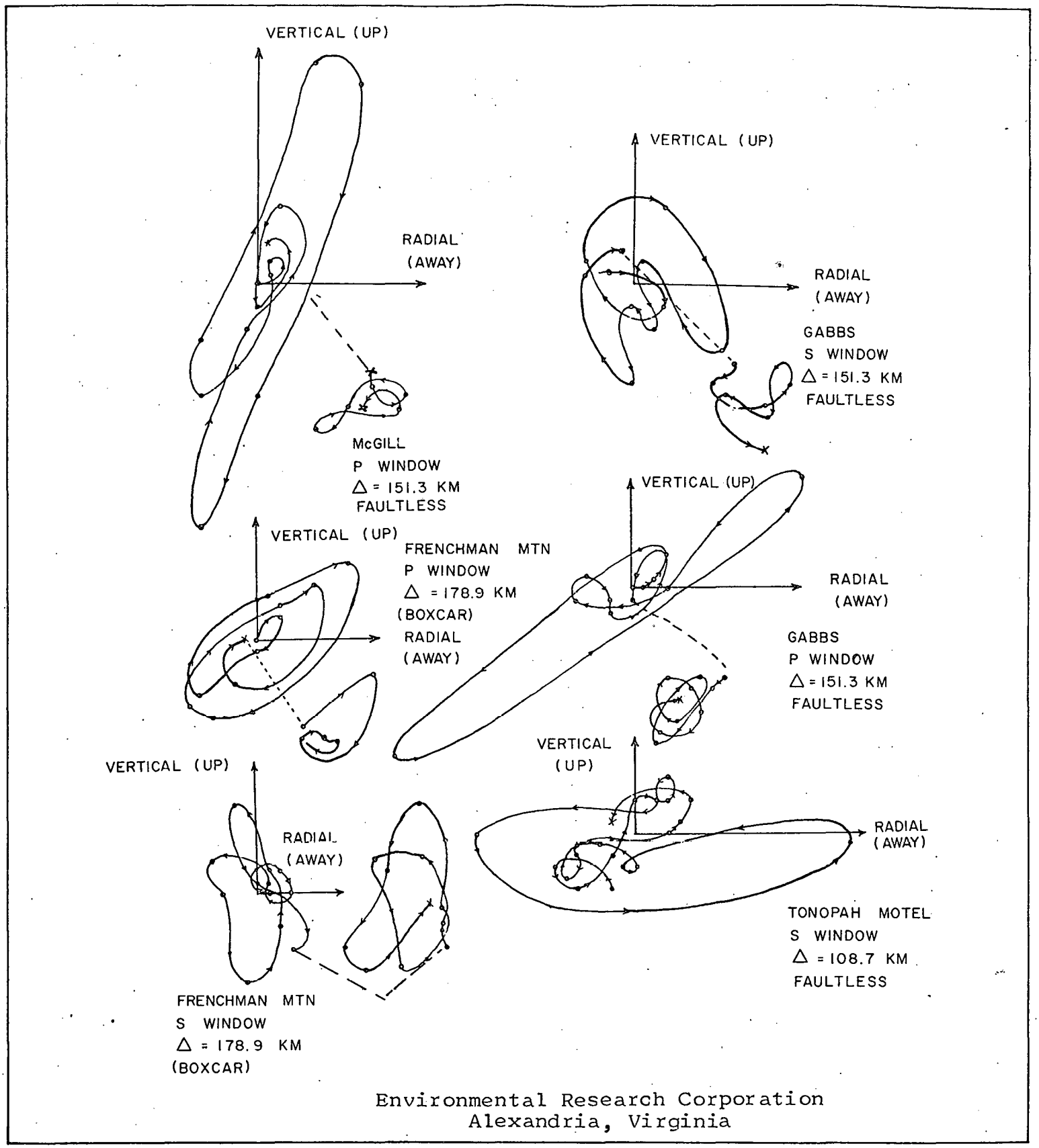

Figure 4-17. Particle Motion Diagrams of P and S Waves Recorded at Selected Stations - Faultless and Boxcar Events. (One-half second intervals)

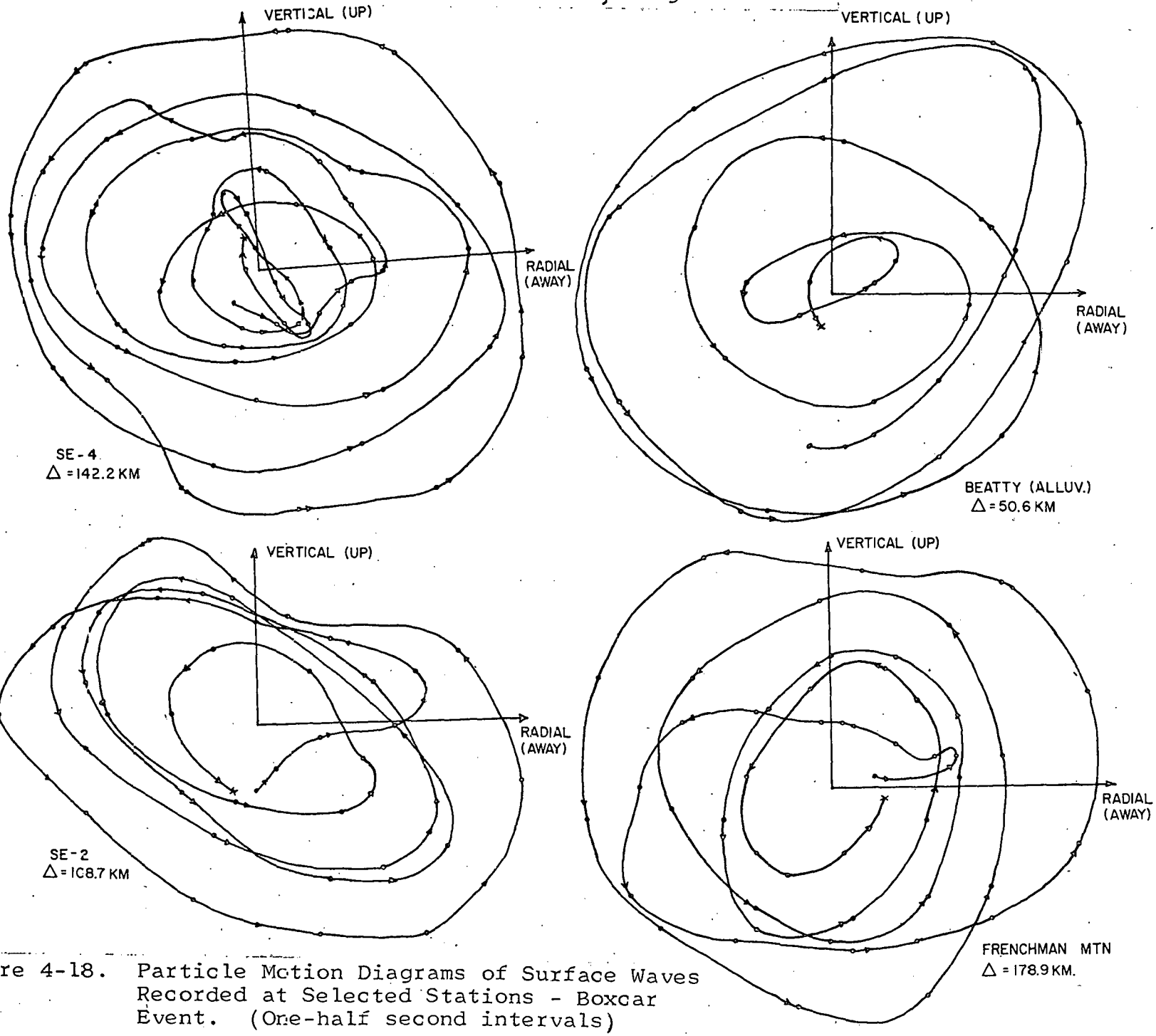

Figure 4-18. Particle Motion Diagrams of Surface Waves Recorded at Selected Stations - Boxcar Event. (One-half second intervals)

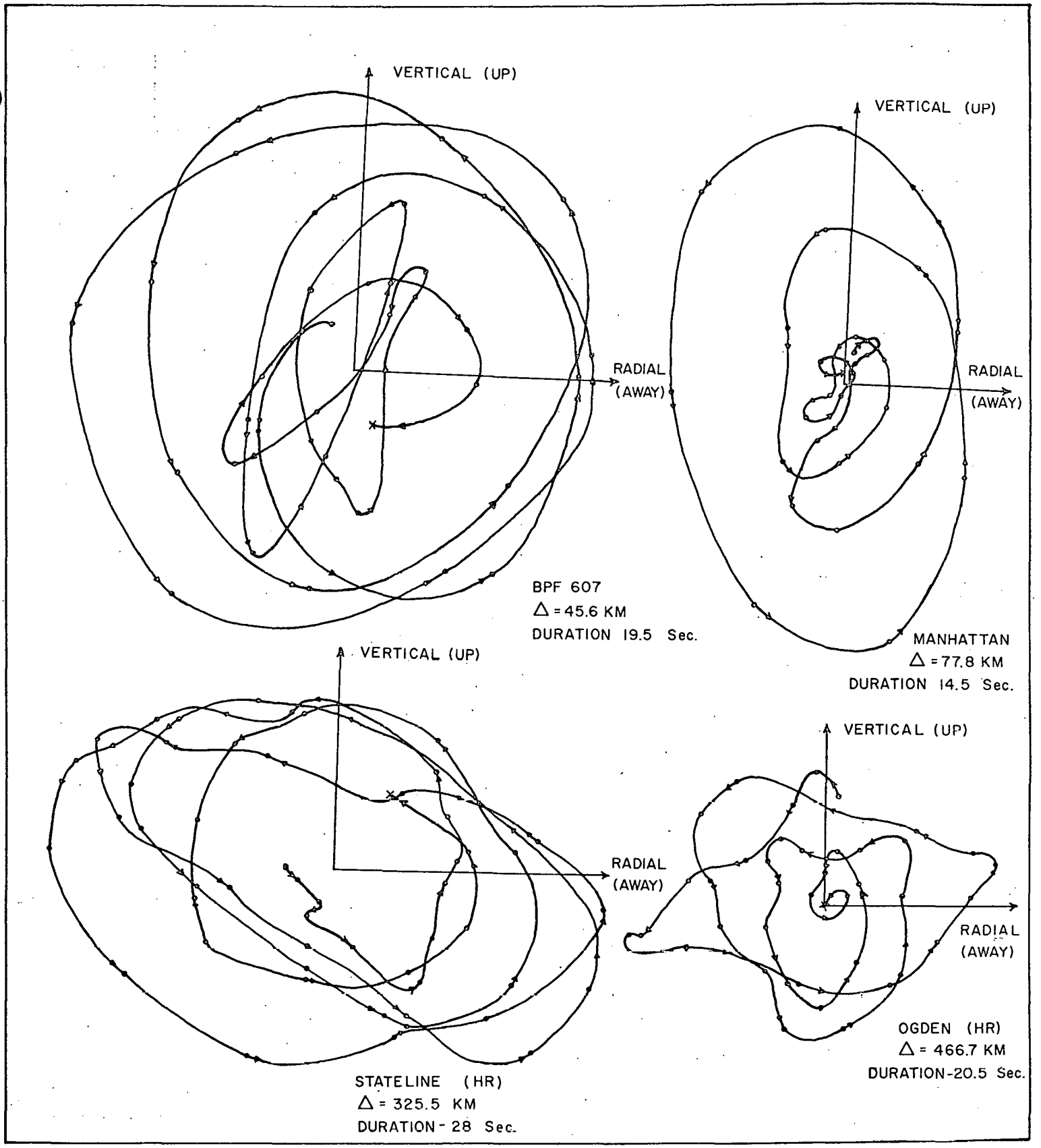

Figure 4-19. Particle Motion Diagrams of Surface Waves Recorded at Selected Stations - Faultless Event. (One-half second intervals)
Environmental Research Corporation
Alexandria, Virginia

CHAPTER 5

CONCLUSIONS AND DIRECTIONS OF FUTURE STUDY

Travel time information, particle motion diagrams (hodographs) and the radial-vertical component product waveform obtained from an analog computer operation all provide useful information which can be used to identify elastic waves on a seismogram. Travel time data provide information on the propagation velocity of the direct and refracted P waves, the parameters of the structured sequence of layers comprising the earth's crust, and a first order estimate of the expected arrival time of S waves having corresponding travel paths. Particle motion diagrams provide a graphic illustration of the actual particle motion recorded and permit a comparison with the particle motion expected for an ideal elastic wave. The radial-vertical component product waveform provides a quick and practical means for identifying P, SV, and Rayleigh waves on most seismograms. In all cases, the certainty of the identification is improved through use of the product waveform, for it is based on the most diagnostic characteristic of an elastic wave, its particle motion.

Examples of typical seismograms recorded from the Boxcar and Faultless events illustrate the complex effect which the heterogeneous nature of the earth's crust has on the recorded seismic waveform. The radial-vertical component product waveform deviates substantially in most cases from the ideal waveform expected from theory. Also, the frequency content shifts noticeably from higher to lower frequencies with increase in time on the seismogram.

Several studies related to the identification of elastic waves on seismograms of underground nuclear explosions are planned for the future. The objective of these studies is to develop the capability to predict the characteristics of the ground motion expected at a station in terms of a specific elastic wave type. Some of the subjects slated for future detailed study which will contribute to this objective are as follows:

1. The spectral character of elastic waves generated by underground nuclear explosions.

2. The attenuation rate of the amplitude associated with specific elastic wave arrivals as a function of distance and yield.

3. The significance of the converted wave on a seismogram.

4. The amplitude relationships of the reflected and refracted waves in the region between the critical point and the critical distance. In particular, the question of possible reinforcement of amplitude by the superposition of two or more waves arriving simultaneously will be studied.

5. Dispersion of surface waves.

Effort to add additional knowledge of the parameters of the earth's crust to existing models will be continued. Also, emphasis will continue to be placed on developing rapid and practical diagnostic techniques for elastic wave identification.

REFERENCES

Berry, R. H., Hays, W. W., Davis, L. L., and Lahoud, J. A., 1968, Analysis of Seismic Data - Faultless Event, Environmental Research Corporation report NVO-1163-154, CONF/FRD.

Bishop, R. H., 1963, Spherical Shock Waves from Underground Explosions, Sandia Corporation report, SC-4907(RR), Section 4.

Bullen, K.E., 1959, An Introduction to the Theory of Seismology, Cambridge University Press.

Cassity, C. R., 1966, Calculation of Earth Motions from an Underground Nuclear Detonation, Environmental Research Corporation report NVO-1163-97.

Cherry, J. T., and Hurdlow, W. R., 1966, Numerical Simulation of Seismic Disturbances, Geophysics, V. 31, p. 33.

Diment, W.H., Stewart, S. W., and Roller, J. C., 1961, Crustal Structure from the Nevada Test Site to Kingman, Arizona from Seismic and Gravity Observations, Journal of Geophysical Research, V. 66, p. 201.

Dobrin, M., 1960, Introduction to Geophysical Prospecting, McGraw-Hill Book Co.

Ewing, W. M., Jarketsky, W. S., and Press, F., 1956, Elastic Waves in Layered Media, McGraw-Hill Book Co.

Grant, F. S., and West, G. G., 1965, Interpretation Theory in Applied Geophysics, McGraw-Hill Book Co.

Hill, D. P., and Pakiser, L. C., 1967, Seismic Refraction Study of Crustal Structure Between the Nevada Test Site and Boise, Idaho, Geological Society of America Bull., V. 78, p. 685.

Holzer, F., 1965, Measurements and Calculations of Peak Shock-Wave Parameters from Underground Nuclear Detonations, Journal of Geophysical Research, V. 70, p. 893.

Love, A.E.H., 1911, Some Problems of Geodynamics, Cambridge University Press.

Lynch, R., 1965, Analog Computer Analysis of Magnetic Tape Seismograms, Environmental Research Corporation report NVO-1163-41.

Oliver, J.P., Pomeroy, P.W., and Ewing, M., 1960, Long Period Seismic Waves from Nuclear Explosions in Various Environments, Science, V. 131, p. 1804.

Press, F., 1960, Crustal Structure in the California - Nevada Region, Journal of Geophysical Research, V. 65, p. 1039.

Rayleigh, J.W.S., 1885, On Waves Propagated Along the Plane Surface of an Elastic Solid, Proc. London Math. Society, V. 17, p. 4.

Reily, D. and Cushing, V., 1967, Characteristic Emissions from an Underground Explosion, Engineering Physics Co. report, DA-49-146-XZ-089.

Ryall, A. and Stuart, D.J., 1963, Travel Times and Amplitudes from Nuclear Explosions, Nevada Test Site to Ordway, Colorado, Journal of Geophysical Research, V. 68, p. 5821.

Sutton, G.H., Mitronovas, W., and Pomeroy, P.W., 1967, Short-Period Seismic Energy Radiation Patterns from Underground Nuclear Explosions and Small-Magnitude Earthquakes, Bulletin of the Seismological Society of America, V. 57, p. 249.

Sutton, G.H., and Pomeroy, P.W., 1963, Analog Analysis of Seismograms Recorded on Magnetic Tape, Journal of Geophysical Research, V. 68, p. 2791.

Yacoub, N.K., Scott, J.H., and McKeown, F.A., 1968, Computer Technique for Tracing Seismic Rays in Two-Dimensional Geological Models, United States Geological Survey, Special Projects Branch Interagency Report NTS-7 (Official Use Only).

Distribution - NVO-1163-157

Mr. D.H. Edwards, AEC/NVOO, Las Vegas, Nevada (3 copies)
Dr. G.H. Higgins, LRL, Livermore, California (1 copy)
Dr. H.L. Reynolds, LRL, Livermore, California (1 copy)
Dr. G.C. Werth, LRL, Livermore, California (1 copy)
Mr. Robert Loux, AEC/NVOO, Las Vegas, Nevada (1 copy)
AEC/DOS, Hq., Washington, D.C. (2 copies)
Mr. J.S. Kelly, AEC/DPNE, Hq., Washington, D.C. (1 copy)
Mr. J.F. Philip, AEC, Berkeley, California (1 copy)
AEC/DMA, Hq., Washington, D.C. (2 copies)
Mr. P.L. Russell, USBM, Denver, Colorado (1 copy)
Dr. W.E. Ogle, LASL, Los Alamos, New Mexico (1 copy)
Mr. R.W. Newman, LASL, Los Alamos, New Mexico (1 copy)
Dr. M.L. Merritt, Org. 5412, Sandia Corp., Albuquerque, New Mexico (1 copy)
Dr. W.D. Weart, Org. 5412, Sandia Corp., Albuquerque, New Mexico (1 copy)
DTIE, Oak Ridge, Tennessee (3 copies)
Dr. W.S. Twenhofel, USGS, Denver, Colorado (1 copy)
Dr. John A. Blume, John A. Blume & Associates, San Francisco, California (2 copies)
Mr. Richard Hamberger, AEC/DPNE, Hq., Washington, D.C. (1 copy)
Dr. Fred Holzer, LRL, Livermore, California (1 copy)
Mr. L.E. Rickey, H&N, Las Vegas, Nevada (1 copy)
Mr. K.W. King, USC&GS, Las Vegas, Nevada (2 copies)
Dr. L.B. Werner, Isotopes, Inc., Palo Alto, California (2 copies)
Mr. T.F. Thompson, San Francisco, California (1 copy)
Dr. N.M. Newmark, University of Illinois, Urbana, Illinois (1 copy)
Mr. S.D. Wilson, Shannon & Wilson, Inc., Seattle, Washington (1 copy)
Dr. D.U. Deere, University of Illinois, Urbana, Illinois (1 copy)
Dr. L.S. Jacobsen, AEC, Los Angeles, California (1 copy)
Dr. G.B. Maxey, University Station, Reno, Nevada (1 copy)
Dr. L.G. vonLossberg, Sheppard T. Powell & Associates, Baltimore, Maryland (1 copy)
Dr. Benjamin Grote, TCD-B, DASA, Sandia Base, Albuquerque New Mexico (2 copies)
Mr. William H. McMaster, LRL, Livermore, California (1 copy)
Mr. H. Carter, SNPO, P.O. Box 1, Jackass Flats, Nevada 89023 (1 copy)
Environmental Research Corporation, Las Vegas, Nevada (2 copies)
Environmental Research Corporation, Alexandria, Virginia (3 copies)